Mimetic Discretizations for Maxwell's Equations and the Equations of Magnetic Diffusion

James M. Hyman and Mikhail Shashkov
Los Alamos National Laboratory
T-7, MS-B284
Los Alamos NM 87545

Subject Classification Numbers: 65N06, 65P05, 77C10
Keywords: Maxwell's Equations, Mimetic Finite Difference Methods, Discrete Vector Analysis, Numerical Methods

Abstract. We have constructed reliable finite difference methods for approximating the solution to Maxwell's equations and the equations of magnetic field diffusion using accurate discrete analogs of differential operators that satisfy the identities and theorems of vector and tensor calculus in discrete form. The numerical approximation does not have spurious modes and mimics many fundamental properties of the underlying physical problem including conservation laws, symmetries in the solution, and the nondivergence of particular vector fields. Numerical examples demonstrate the high-quality of the method when the media is strongly discontinuous and for nonorthogonal, nonsmooth computational grids.

1. Introduction. We are developing a discrete analog of vector and tensor calculus that can be used to accurately approximate continuum models for a wide range of physical processes on logically rectangular, nonorthogonal, nonsmooth grids. These finite difference methods (FDMs) preserve fundamental properties of the original continuum differential operators and allow the discrete approximations of partial differential equations (PDEs) to mimic critical properties including conservation laws and symmetries in the solution of the underlying physical problem. The discrete analogs of differential operators satisfy the identities and theorems of vector and tensor calculus and provide new reliable algorithms for a wide class of PDEs [21]-[24]. This approach has been used to construct high-quality mimetic FDMs for the divergence and gradient in approximating the diffusion equation [25], [48], [49]. In this paper we apply our new methodology to construct mimetic FDMs to Maxwell's first-order curl equations (hyperbolic type) and the equations of magnetic diffusion (parabolic type).

The system of first-order Maxwell's curl equations

$$\frac{\partial \vec{B}}{\partial t} = -\mathbf{curl}\, \vec{E}\,, \tag{1.1-a}$$

$$\frac{\partial \vec{E}}{\partial t} = \frac{1}{\epsilon}\, \mathbf{curl}\, \frac{\vec{B}}{\mu}\,, \tag{1.1-b}$$

model the evolution of magnetic and electric fields. Here $\vec{B}$ is the magnetic flux density, $\vec{E}$ is the electric field intensity, ϵ is the permitivity, and μ is the permeability. The parameters are in general symmetric positive definite tensors with possibly discontinuous elements at the interface between different media.

We have chosen this form for the equations because at the interface between two media the normal components of $\vec{B}$ and the tangential components of $\vec{E}$ are continuous (see for example, [44]). The FDM will use exactly these vectors components to describe the magnetic and electric fields.

In addition to equations 1.1-a, 1.1-b, the following "divergence-free" conditions

$$\mathbf{div}\, \vec{D} = 0\,, \tag{1.2-a}$$

$$\mathbf{div}\, \vec{B} = 0\,, \tag{1.2-b}$$

must be satisfied. Here $\vec{D} = \epsilon\, \vec{E}$ is the electric flux density.

If the "divergence-free" conditions are satisfied initially by the solution of 1.1-a, 1.1-b, then they will be satisfied at later times. This is easily shown by taking the divergence of these equations and using the fact that $\mathbf{div}\,\mathbf{curl} \equiv 0$. If the discrete operators also satisfy this property then we can use only the discrete analogs of equations 1.1-a, 1.1-b in our numerical method, because discrete analogs of equations 1.2-a, 1.2-b will also be the consequence of the discrete "curl" equations.

In our FDM $\vec{B}$ and $\vec{E}$ are the primary variables and the governing equations are discretized as a system of two first-order equations. We define the tensors determining material properties in the grid cells, and assume that the interface between different materials coincides with the faces of the cells (edges in 2D). Also because we use different discrete description of the magnetic and electric fields we need two different discrete analogs of **curl**.

The first governing equation 1.1-a is a differential form of Faraday' law of electromagnetic induction:

$$\frac{d}{dt} \int_S (\vec{B}, \vec{n})\, dS = -\oint_L (\vec{E}, \vec{l})\, dl\,. \tag{1.3}$$

Here S is the surface spanning (based on) the closed curve L, $\vec{n}$ is the unit outward normal to S, and $\vec{l}$ is the unit tangential vector to the curve l.

To create the discrete analog of the law of electromagnetic induction, we define the discrete curl using the coordinate invariant definition of the $\mathbf{curl}\,\vec{E}$ based on Stoke's circulation theorem,

$$(\vec{n}, \mathbf{curl}\,\vec{E}) = \lim_{S \to 0} \frac{\oint_L (\vec{E}, \vec{l})\, dl}{S} \,. \tag{1.4}$$

In the discrete case the faces of the grid cells will be the surfaces S in equation 1.4 and the "curve" L will be formed by edges of the cell. Equation 1.4 naturally defines the domain for the discrete analog of $\mathbf{curl}\,\vec{E}$ as the tangential components of $\vec{E}$ given on edges (orthogonal projections of $\vec{E}$ onto the directions of the edges). The natural range of values will be the normal components of $\mathbf{curl}\,\vec{E}$ given on the faces of the cells (orthogonal projections of $\mathbf{curl}\,\vec{E}$ onto the directions of the normals to the cell faces).

This definition of the discrete analog of $\mathbf{curl}\,\vec{E}$ and equation 1.1-a naturally leads to using the normal components of $\vec{B}$ to describe the magnetic field in the discrete case (recall that they are continuous at interfaces). That is, the discrete analogs of both sides of 1.1-a belong to the same discrete space, and we do not need to interpolate between the spaces. This construction preserves a discrete analog of Faraday's law of electromagnetic induction locally for each face.

When discretizing equation 1.1-b, when ϵ and μ are discontinuous and (or) the computational grid is not smooth, then it is not possible to separate the discretization of $\mathbf{curl}\,\vec{B}$ from the discretization of $\frac{1}{\epsilon}\,\mathbf{curl}\,\frac{\vec{B}}{\mu}$. Therefore we will construct discrete analog of the full operator $\frac{1}{\epsilon}\,\mathbf{curl}\,\frac{\vec{B}}{\mu}$ using the integral identity for curls

$$\int_V (\vec{H},\, \mathbf{curl}\,\vec{E})\, dV - \int_V (\vec{E},\, \mathbf{curl}\,\vec{H})\, dV = \oint_{\partial V} ([\vec{E} \times \vec{H}],\, \vec{n})\, dS \,. \tag{1.5}$$

This identity is responsible for the law of conservation of electromagnetic energy:

$$\frac{d}{dt} \int_V \frac{1}{2} \left\{ (\vec{E},\, \vec{D}) + (\vec{B},\, \vec{H}) \right\} dV = - \oint_{\partial V} ([\vec{E} \times \vec{H}], \vec{n})\, dS \,, \tag{1.6}$$

where $\vec{H} = \frac{\vec{B}}{\mu}$ is the magnetic field density. This approach will guarantee that the electromagnetic energy is conserved on the discrete level.

To form the operator $\frac{1}{\epsilon}\,\mathbf{curl}\,\frac{\vec{B}}{\mu}$ we rewrite the identity 1.5 as

$$\int_V \frac{1}{\mu} (\vec{B},\, \mathbf{curl}\,\vec{E})\, dV - \int_V \epsilon\, (\vec{E},\, \frac{1}{\epsilon}\, \mathbf{curl}\, \frac{\vec{B}}{\mu})\, dV = \oint_{\partial V} \frac{1}{\mu} ([\vec{E} \times \vec{B}],\, \vec{n})\, dS \,, \tag{1.7}$$

and use this identity to construct a discrete analog of $\frac{1}{\epsilon}\,\mathbf{curl}\,\frac{\vec{B}}{\mu}$ within the framework of the support-operators method (SOM) [45, 46, 48]. In the SOM, first a discrete approximation is defined for a first-order differential operator, such as the divergence or gradient, that satisfies the appropriate discrete analog of an integral identity, such as Stokes' theorem. This initial discrete operator, called the *prime* operator, then *supports* the construction of the other discrete operators, using discrete formulations of the integral identities. For example, if $\mathbf{curl}\,\vec{E}$ is discretized directly and then the discrete analog of 1.7 and the prime operator is used to derive the discrete analog of the operator $\frac{1}{\epsilon}\,\mathbf{curl}\,\frac{\vec{B}}{\mu}$. By construction, the domain of this discrete operator is the normal components of vector given on the grid cell faces, and the range of values is the tangential components on the cell edges.

We now consider how to discretize the "divergence-free" conditions so they follow from the discrete curl equations. To discretize the condition $\mathbf{div}\,\vec{B} = 0$ we will use the natural coordinate invariant definition of the divergence based on Gauss' divergence theorem;

$$\mathbf{div}\,\vec{B} = \lim_{V\to 0} \frac{\oint_{\partial V} (\vec{B}, \vec{n})\, dS}{V} \,. \tag{1.8}$$

The domain of this discrete divergence is the normal components of the vector given on the faces and the range of values is scalars given in the cells. It is shown in [21] that this discrete divergence satisfies the discrete analog of identity $\mathbf{div}\,\mathbf{curl}\,\vec{E} = 0$ in each cell. Therefore if a discrete analog of $\mathbf{div}\,\vec{B} = 0$ holds initially, then it will hold for later times.

To discretize the condition $\mathbf{div}\,\vec{D} = \mathbf{div}\,\epsilon\,\vec{E} = 0$, we need to define a discrete analog of operator $\mathbf{div}\,\epsilon\,\cdot$ with a domain consisting of the tangential components of the vectors. In [22] we constructed a discrete $\mathbf{div}$ with this domain using the integral identity

$$\int_V (\vec{W}, \mathbf{grad}\ u)\, dV = -\int_V u\, \mathbf{div}\, \vec{W}\, dV + \oint_{\partial V} u\, (\vec{W}, \vec{n})\, dS \,, \tag{1.9}$$

where we considered the case when the boundary integral is equal to zero (see, [22]).

To discretize the operator $\mathbf{div}\,\epsilon\,\cdot$ we first define a natural discrete gradient and then use the SOM and the identity

$$\int_V \epsilon(\vec{W}, \mathbf{grad}\ u)\, dV = -\int_V u\, \mathbf{div}\, \epsilon\, \vec{W}\, dV \,. \tag{1.10}$$

For any direction l given by the unit vector $\vec{l}$, the directional derivative can be defined as

$$\frac{\partial u}{\partial l} = (\mathbf{grad}\, u, \vec{l}) \,. \tag{1.11}$$

This definition applied to the edges of the cell will define a natural discrete gradient with the domain containing scalar functions at the nodes and range of values given by the tangential components of a vector function on the cell edges. The discrete gradient defines a discrete analog of $\mathbf{div}\,\epsilon\,\cdot$ satisfying discrete analog of 1.10 with the desired domain and range of values. The range of values are nodal scalar functions and the discrete analog of the condition $\mathbf{div}\,\vec{D} = 0$ holds at the nodes. Similar to [22] we will prove that these operators satisfy a discrete analog of the identity $\mathbf{div}\,\mathbf{curl}\,\vec{H} = 0$. That is, in terms of our primary variables,

$$\mathbf{div}\,\epsilon * \frac{1}{\epsilon}\,\mathbf{curl}\,\frac{\vec{B}}{\mu} = 0 \,.$$

Therefore if discrete analog of $\mathbf{div}\,\epsilon\vec{E} = 0$ holds initially it will hold for any time.

Using these discrete spatial operators we obtain a conservative semi-discrete method, where time is still continuous. If we denote discrete operators using capital letters, then the semi-discrete equations are

$$\frac{\partial \vec{B}}{\partial t} = -\mathrm{CURL}\, \vec{E}\,, \tag{1.12-a}$$

$$\frac{\partial \vec{E}}{\partial t} = {}_{\epsilon}\overline{\mathrm{CURL}}_{\mu}\, \vec{B}\,, \tag{1.12-b}$$

We consider time discretization methods of the form

$$\frac{\vec{B}^{n+1} - \vec{B}^{n}}{\Delta t} = -\mathrm{CURL}\, \vec{E}^{\alpha_1}\,, \tag{1.13-a}$$

$$\frac{\vec{E}^{n+1} - \vec{E}^{n}}{\Delta t} = {}_{\epsilon}\overline{\mathrm{CURL}}_{\mu}\, \vec{B}^{\alpha_2}\,, \tag{1.13-b}$$

where $\vec{E}^{\alpha_1} = \alpha_1\, \vec{E}^{n+1} + (1-\alpha_1)\, \vec{E}^{n}$ and $\vec{B}^{\alpha_2} = \alpha_2\, \vec{B}^{n+1} + (1-\alpha_2)\, \vec{B}^{n}$, and $t_n = \Delta t\, n$. It is easy to show that the explicit schemes ($\alpha_1 = 0$ or $\alpha_2 = 0$) do not preserve energy. For some problems with strongly discontinuous coefficients, it is important to preserve energy. The only method of this form which preserves energy is the midpoint method ($\alpha_1 = \alpha_2 = 0.5$). We will describe how approach to solve system of linear equations arising when using this implicit scheme. The adjointness property of the discrete curls guarantees that system linear equations will be symmetric and positive definite (SPD).

We will also consider the parabolic equations of magnetic diffusion [18], [20], [51]

$$\frac{\partial \vec{B}}{\partial t} = -\mathbf{curl}\, \vec{E}\,, \tag{1.14-a}$$

$$\vec{E} = \frac{1}{\sigma}\, \mathbf{curl}\, \frac{\vec{B}}{\mu}\,, \tag{1.14-b}$$

which arise in magnetohydrodynamics (MHD). Here the conductivity σ can be symmetric positive definite discontinuous tensor. For these equations we use the same description of the magnetic and electric fields and the same discretizations for the spatial operators as we do for Maxwell's curl equations. The conductivity σ plays the same role as ϵ.

The equations of magnetic diffusion are often solved together with Lagrangian hydrodynamics. The Lagrangian grids move with the media and can be extremely distorted or rough; FDMs have to be robust and accurate on these grids. Implicit time integration methods are required to efficiently solve these equations in many practical applications. When integrating the equations with an implicit method our approach guarantees that the system of linear equations is SPD even on highly distorted grids. The SPD property allows powerful iterative methods to be used to solve these equations. Numerical examples presented in Section 7 demonstrate that the FDMs are also accurate nonsmooth grids.

There is a huge literature related to solving Maxwell's equations. Traditional node-based finite-difference and finite-element method are described in [7], [18]. [28]. One of the most widely used and effective numerical method for solving the time-dependent electromagnetic problems is the finite-difference time-domain (FDTD) method developed by Yee, [54], (see also [52], p. 59–61). The original Yee method solves the two first-order curl equations for magnetic and electric field as primary variables and is identical to our method in the special case of rectangular grids. Recently Yee's method has been extended for general grids [33], [52]. pp. 369–374. In this generalization the electric field is described by the tangential components on the edges of the grid, as in our method. However, this generalization uses the tangential components of the magnetic field with respect to the edges of the dual grid, obtained by connecting centers of cells of original grid. In contrast, we use the normal components of magnetic field with respect to the faces of the original grid.

Our description of magnetic field overcomes several of the disadvantages of the generalized Yee method used in [52]. First, the direction of the vector connecting the centers of the cells does not coincide with the normals to the cell faces. Therefore when $\vec{H}$ is not continuous as whole vector, the components related to this direction are discontinuous and the discretization introduces unremovable errors. Also, the range of values of the discrete analog of $\mathbf{curl}\,\vec{E}$ does not coincide with the domain of $\mathbf{curl}\,\vec{H}$ and therefore either $\vec{H}$ or $\vec{E}$ must be interpolated. When ϵ and (or) μ are discontinuous the interpolation can introduce large errors. Even when these quantities are continuous the interpolation can introduce spurious modes into the solution [27]. Next, because the definitions of the discrete curls are incompatible, the electromagnetic energy is not conserved. And finally, in the situation where implicit scheme is used the resulting system of linear equations is not SPD. By using the components of magnetic field normal to faces of original grid all these problems are resolved.

For general problems, the FDM and analysis is presented here for the first time. However for the equations of magnetic diffusion Shashkov and others published a series of papers (independent of Yee's paper) constructing variational FDMs on logically rectangular girds [30]-[32]. For this particular problem the discretization and location of variables is the same as the method we are proposing. The discretizations of the curl operator constructed in these papers have been applied to the solutions of Maxwell's equations in cylindrical geometry on orthogonal grids [14] and to modeling a microwave plasma generator [36]. The stability and convergence of the variational FDMs have been theoretically analyzed [4], using the energy method based on the adjointness property of the discrete operators.

The finite-element method (FEM) [28], [50], [12] has been used extensively to solve Maxwell's equations. The "spirit" of our FDM is close to the original mixed FEM introduced by Raviart and Thomas, [43], and Nedelec, [42], [1]. In [42] (p. 334), in particular, Nedelec noted that "it is natural to approximate $\vec{E}$ in $H(\mathbf{curl})$ and $\vec{B}$ in $H(\mathbf{div})$". In our FDM we use the discrete analogs of these spaces. The innovative ideas in [42] lead to introducing so called vector elements (see, for example, [28], Chapter 8, pp. 231–280) for solving Maxwell's equations. Surprisingly, however, many practitioners only use edge vector elements (space $H(\mathbf{curl})$ to discretize second-order equations for electric or magnetic field [28], [53], [2]. Although, there have been some attempts to mix both normal and tangential vector elements in one interpolant [10].

Algebraic topology provides a natural framework to describe discrete structures (e.g. [16], [15], and references in [21]). By applying this approach to electromagnetics, [5], [6], [29]), formal structures can be introduced that correspond to the objects of electromagnetics. In [5] the "edge elements" and "facet elements" are introduced that correspond to our discretization of the electric and magnetic fields have been introduced. Similar constructions have been used [37] to uniformly describe FEMs, FDMs and finite-volume methods. The ideas of algebraic topology have been applied to developing numerical methods (especially on rectangular grids) for more then forty years (see references in [21]). The main problem in this approach is in the construction of consistent adjoint operators. This paper, and [21]-[24] provides a self-consistent FDM based on the discrete vector analysis without using any terminology or ideas from algebraic topology.

There is continuing discussion about the origin of spurious solutions that arise min computational electromagnetic models (e.g. [27] is totally devoted to this problem, and [35], [3]). Spurious solutions for FDMs for first-order systems can originate from inconsistent discretizations of the operators **div**, **curl**, and **grad**. SOM FDMs defined in consistent way are free of spurious solutions. In [21] and [22], we proved discrete analogs of main theorems of vector analysis for SOM FDMs. These theorems include Gauss' theorem; the theorem that $\mathbf{div}\,\vec{A}=0$ if and only if $\vec{A}=\mathbf{curl}\,\vec{B}$; $\mathbf{curl}\,\vec{A}=0$ if and only if $\vec{A}=\mathbf{grad}\varphi$; the theorem that if $\vec{A}=\mathbf{grad}\,\varphi$, then line integral does not depend on path; and the theorem that if the line integral of a vector function is equal to zero for any closed path, then this vector is the gradient of a scalar function. In [23] we proved discrete analogs of the orthogonal decomposition theorem for the discretization of a vector field. That is, for given discrete divergence and curl, a discrete vector can be decomposed into two orthogonal vectors in unique way satisfying a discrete analog of the formula $\vec{A}=\mathbf{grad}\,\varphi+\mathbf{curl}\,\vec{B}$, if its normal or tangential component is given on the boundary. The discrete orthogonal decomposition theorem is proven for vectors described by the tangential components on the edges (as is the electric field in this paper), and for vectors described by normal components on the faces (as is magnetic field in this paper).

In Section 2 we give a brief review of basic electromagnetics and discuss the properties of the governing equations. We the illuminate properties of the differential operators we preserve in our discrete model. In Sections 3 and 4 we summarize the results from [21]-[22] needed to prove these properties. After describing the grid, the discretizations of scalar and vector functions, and the inner products in the discrete function spaces, we review the derivation of the natural and adjoint finite difference analogs for the divergence, gradient, and curl and introduce discrete analogs of operators $\mathbf{div}\,\epsilon\,\cdot$ and $\frac{1}{\epsilon}\,\mathbf{curl}\,\frac{\cdot}{\mu}$. We also consider the discrete analogs of the theorems of vector analysis needed for the derivations in this paper. In Section 5 we describe our FDMs and prove that they satisfy the desired properties. In Section 6 we discuss the solution of implicit equations. Finally in Section 7, we present the numerical examples.

2. A Brief Review of Basic Electromagnetics.

2.1. The General Differential Form.

For general time-varying fields, Maxwell's equations in differential form can be written as

$$\frac{\partial \vec{B}}{\partial t}=-\mathbf{curl}\,\vec{E}\,,\quad \text{(Faraday's law)}\,, \tag{2.1-a}$$

$$\frac{\partial \vec{D}}{\partial t}=\mathbf{curl}\,\vec{H}-\vec{J},\quad \text{(Maxwell-Ampére law)}\,, \tag{2.1-b}$$

$$\mathbf{div}\,\vec{D}=\rho\,,\quad \text{(Gauss's law)}\,, \tag{2.1-c}$$

$$\mathbf{div}\,\vec{B}=0\,,\quad \text{(Gauss's law – magnetic)}\,, \tag{2.1-d}$$

where $\vec{E}$ = electric field intensity, $\vec{D}$ = electric flux density, $\vec{H}$ = magnetic field density, $\vec{B}$ = magnetic flux density, $\vec{J}$ = electric current density, and ρ = electric charge density.

Also, the conservation of charge is governing by the continuity equation

$$\mathbf{div}\,\vec{J} = -\frac{\partial \rho}{\partial t}\,. \tag{2.2}$$

Only three of the equations 2.1-a-2.2 are independent. Usually either 2.1-a-2.1-c, or 2.1-a, 2.1-b and 2.2 are chosen as the independent equations. The remaining dependent equations can be derived from the independent equations.

2.2. Constitutive Relations. Because the number of equations is less than the number of unknowns, either choice for the three independent equations is indefinite. Maxwell's equations become definite when the constitutive relationships between the field quantities describing the macroscopic properties of the medium are specified. For a simple medium, they are

$$\vec{D} = \epsilon\,\vec{E}\,, \tag{2.3-a}$$
$$\vec{B} = \mu\,\vec{H}\,, \tag{2.3-b}$$
$$\vec{J} = \sigma\,\vec{E}\,, \tag{2.3-c}$$

where the constitutive parameters $\epsilon\,,\mu$ and σ denote, respectively, the permitivity, permeability, and conductivity of the medium. These parameters are tensors for anisotropic media and scalars for isotropic media. For inhomogeneous media, they are also functions of position.

2.3. Conditions on the Interface between Two Media. If neither surface currents nor surface charges exist at the interface between two media, say medium 1 and medium 2, then the boundary conditions for the electric field can be expressed as

$$\vec{n} \times (\vec{E}_1 - \vec{E}_2) = 0\,, \tag{2.4-a}$$
$$(\vec{n},\,(\vec{D}_1 - \vec{D}_2)) = 0\,, \tag{2.4-b}$$

and the boundary conditions for the magnetic filed are

$$\vec{n} \times (\vec{H}_1 - \vec{H}_2) = 0\,, \tag{2.5-a}$$
$$(\vec{n},\,(\vec{B}_1 - \vec{B}_2)) = 0\,. \tag{2.5-b}$$

Here $\vec{n}$ is the unit vector normal to the interface pointing from medium 2 to into medium 1.

If there is a surface electric current density, $\vec{J}_s$, and a surface charge density, ρ_s, then equations 2.4-b and 2.5-a must be modified to

$$(\vec{n},\,(\vec{D}_1 - \vec{D}_2)) = \rho_s\,, \tag{2.6-a}$$
$$\vec{n} \times (\vec{H}_1 - \vec{H}_2) = \vec{J}_s\,. \tag{2.6-b}$$

Because ρ_s and $\vec{J}_s$ are in general unknown, the conditions 2.6-a and 2.6-b do not provide any useful information.

However, from 2.4-a and 2.5-b it follows that the tangential components of $\vec{E}$ and normal components of $\vec{B}$ are continuous at the medium interface. We will use this fact and use these quantities to describe the electric and magnetic fields in the discrete case.

2.4. Governing Equations. In this paper we will use equations 2.1-a, 2.1-b and 2.2 as our independent equations.

2.4.1. Maxwell's curl Equations. We first consider a nonconducting, ($\sigma = 0 \Longrightarrow \vec{J} = \sigma\vec{E} = 0$), free of charge, ($\rho = 0$) medium. In this case the continuity equation 2.2 always holds, and therefore the governing equations are

$$\frac{\partial \vec{B}}{\partial t} = -\mathbf{curl}\,\vec{E}\,, \tag{2.7-a}$$

$$\frac{\partial \vec{D}}{\partial t} = \mathbf{curl}\,\vec{H}\,, \tag{2.7-b}$$

and the dependent equations are

$$\mathbf{div}\,\vec{D} = 0\,, \tag{2.8-a}$$

$$\mathbf{div}\,\vec{B} = 0\,. \tag{2.8-b}$$

If equation 2.8-b is initially satisfied then it will hold at later times. This follows if we apply **div** to the left- and right-hand sides of 2.7-a and using the identity $\mathbf{div}\,\mathbf{curl}\,\vec{E} = 0$, to obtain

$$\frac{\partial \mathbf{div}\vec{B}}{\partial t} = 0\,; \tag{2.9}$$

therefore $\mathbf{div}\vec{B} = \mathit{const} = \mathbf{div}\vec{B}|_{t=0} = 0$. For similar derivations to be valid for the discrete case, the discrete curl, CURL, and divergence, DIV, must satisfy the identity

$$\mathrm{DIV\ CURL} = 0\,. \tag{2.10}$$

Similarly, if 2.8-a is initially satisfied it will hold at later times. This follows from applying **div** to the left- and right-hand sides of 2.7-b and using the identity $\mathbf{div}\,\mathbf{curl}\,\vec{H} = 0$ to obtain

$$\frac{\partial \mathbf{div}\vec{D}}{\partial t} = 0\,; \tag{2.11}$$

therefore $\mathbf{div}\vec{D} = \mathit{const} = \mathbf{div}\vec{D}|_{t=0} = 0$. Equation 2.8-a follows from the three governing equations and identity $\mathbf{div}\,\mathbf{curl}\,\vec{H} = 0$. For the discrete Gauss' equation to be a consequence of the discrete governing equations the discrete identity DIV CURL $\vec{H}$ must be satisfied.

The discrete analog of the identities $\mathbf{div}\,\mathbf{curl}\,\vec{H} = 0$ and $\mathbf{div}\,\mathbf{curl}\,\vec{E} = 0$ are different when vectors $\vec{H}$ and $\vec{E}$ belong to different spaces. Consequently the discrete analogs of **div** and **curl** must be different in the two identities.

When $\rho = 0\,, \vec{J} = 0$, we need to consider only equations 2.7-a, 2.7-b (if conditions 2.8-b, 2.8-a are satisfied initially then they will be satisfied at later times). Therefore we base our FDM on equations 2.7-a, 2.7-b and require that the discrete analogs of the identities $\mathbf{div}\,\mathbf{curl}\,\vec{H} = 0$, $\mathbf{div}\,\mathbf{curl}\,\vec{E} = 0$ hold *exactly*, and that that discrete analogs of the conditions $\mathbf{div}\,\vec{D} = 0$, $\mathbf{div}\,\vec{B} = 0$ are initially satisfied. Again, because in the discrete case when $\vec{D}$ and $\vec{B}$ belong to different discrete spaces then the discrete divergences and curls in these conditions will be different.

Finally because the normal components of $\vec{B}$ and the tangential components of $\vec{E}$ are continuous across discontinuities in the media, we will use them to describe magnetic and electric fields and discretize the governing hyperbolic equations

$$\frac{\partial \vec{B}}{\partial t} = -\mathbf{curl}\,\vec{E}\,, \tag{2.12-a}$$

$$\frac{\partial \vec{E}}{\partial t} = \frac{1}{\epsilon}\,\mathbf{curl}\,\frac{\vec{B}}{\mu}\,. \tag{2.12-b}$$

We will consider media where both ϵ and μ can be discontinuous tensors. Note that this system can be reduced to a single wave equation for either $\vec{E}$ or $\vec{B}$.

When both ρ and $\vec{J}$ are nonzero, the continuity equation 2.2 provides the important compatibility condition for the solution. And as mentioned in [3] (page 364), "after discretizations, these properties may very well be violated, for example, when the discrete charge and current density ρ_h and J_h are computed from a particle approximation ...". We agree with this observation and note that the problem arise when the model for computation of ρ_h and J_h is not self-consistent. One example of consistent discretization can be found in [36], where the Maxwell's equations are solved together with Vlasov's equations describing the evolution of the electron distribution density function. We require that the distribution of discrete charge and current density satisfy a discrete analog of the continuity equation. There are situations when this condition cannot be satisfied and an alternative approach must be used [3], [27].

2.4.2. Magnetic Diffusion Equations. In many MHD models ([51] p. 24), term $\partial\vec{D}/\partial t$ can be neglected in equation 2.1-b. Consequently, $\partial\rho/\partial t$ can be neglected in the continuity equation and ρ is explicitly defined by

$$\rho = \mathbf{div}\,\vec{D}\,. \tag{2.13}$$

Also, the charge distribution rarely plays a central role in MHD ([51] p. 22) and equation 2.13 can be completely decoupled from the other equations. Furthermore, in MHD the media is often nonmagnetic, that is $\mu = \mu_0$, where $\mu_0 = const$ and the conductivity σ can be a discontinuous tensor.

The independent equations are

$$\frac{\partial\vec{B}}{\partial t} = -\mathbf{curl}\,\vec{E}\,, \tag{2.14-a}$$

$$\vec{J} = \sigma\,\vec{E} = \mathbf{curl}\,\frac{\vec{B}}{\mu}\,, \tag{2.14-b}$$

$$\mathbf{div}\,\vec{J} = 0\,. \tag{2.14-c}$$

Equation 2.14-c is a consequence of 2.14-b (as seen by applying **div** to both sides of 2.14-b) and can be eliminated. This reduces the governing equations to

$$\frac{\partial\vec{B}}{\partial t} = -\mathbf{curl}\,\vec{E}\,, \tag{2.15-a}$$

$$\vec{E} = \frac{1}{\sigma}\,\mathbf{curl}\,\frac{\vec{B}}{\mu}\,. \tag{2.15-b}$$

Also, we can eliminate $\vec{E}$ and obtain the parabolic magnetic field diffusion equation for $\vec{B}$:

$$\frac{\partial\vec{B}}{\partial t} = -\mathbf{curl}\,\frac{1}{\sigma}\,\mathbf{curl}\,\frac{\vec{B}}{\mu}\,. \tag{2.16}$$

2.5. Boundary Conditions. In this paper we consider the case when the tangential component of $\vec{E}$ is given on the boundary

$$\vec{n}\times\vec{E} = \gamma\,. \tag{2.17}$$

When $\gamma = 0$, this condition is appropriate for a perfectly conducting surface. The approximation of 2.17 is especially easy for our FDM because we use the tangential components of $\vec{E}$ to describe the electric field.

Impedance boundary conditions (see [28], p. 7) when a combination of the tangential components of $\vec{E}$ and of $\vec{H}$ given on the boundary can also be treated in framework of our method (see note at the end of section 4.2.3).

2.6. Electromagnetic Energy. The energy density of the electromagnetic field is defined as

$$\frac{1}{2}\left\{(\vec{E}, \vec{D}) + (\vec{B}, \vec{H})\right\} \tag{2.18}$$

for a linear and nondispersive medium where ϵ and μ are independent of the field variables and time. The conservation law in electromagnetics can be formulated as ([44], page 339)

$$-\int_V (\vec{J}, \vec{E})\, dV = \frac{d}{dt}\int_V \frac{1}{2}\left\{(\vec{E}, \vec{D}) + (\vec{B}, \vec{H})\right\}\, dV + \oint_{\partial V} ([\vec{E}\times\vec{H}], \vec{n})\, dS\,, \tag{2.19}$$

where $\vec{n}$ is the unit outward normal to the surface ∂V. This equation can be derived by first taking the scalar product of equation 2.1-b with $\vec{E}$ and subtracting the resulting equation from the scalar product of equation 2.1-a with $\vec{H}$ to obtain

$$(\vec{H}, \mathbf{curl}\,\vec{E}) - (\vec{E}, \mathbf{curl}\, H) = -(\vec{H}, \frac{\partial \vec{B}}{\partial t}) - (\vec{E}, \frac{\partial \vec{D}}{\partial t}) - (\vec{E}, \vec{J})\,. \tag{2.20}$$

Then, using the property

$$\frac{\partial}{\partial d}(\vec{E}, \vec{E}) = 2(\vec{E}, \frac{\partial \vec{E}}{\partial t}) \tag{2.21}$$

and that ϵ and μ are independent of time, we have

$$(\vec{E}, \frac{\partial \vec{D}}{\partial t}) = \frac{\partial}{\partial t}\frac{1}{2}(\vec{E}, \vec{D})\,, \tag{2.22-a}$$

$$(\vec{H}, \frac{\partial \vec{B}}{\partial t}) = \frac{\partial}{\partial t}\frac{1}{2}(\vec{H}, \vec{B})\,. \tag{2.22-b}$$

Next, integrating equation 2.20 over the domain V and using 2.22-a and 2.22-b we obtain

$$\begin{aligned} &\int_V \left\{(\vec{H}, \mathbf{curl}\,\vec{E}) - (\vec{E}, \mathbf{curl}\,\vec{H})\right\}\, dV = \\ &-\frac{d}{dt}\int_V \frac{1}{2}\left\{(\vec{E}, \vec{D}) + (\vec{B}, \vec{H})\right\}\, dV - \int_V (\vec{J}, \vec{E})\, dV\,. \end{aligned} \tag{2.23}$$

The conservation law 2.19 follows from this equation and the identity

$$\int_V (\vec{H}, \mathbf{curl}\,\vec{E})\, dV - \int_V (\vec{E}, \mathbf{curl}\,\vec{H})\, dV = \oint_{\partial V} ([\vec{E}\times\vec{H}], \vec{n})\, dS\,. \tag{2.24}$$

For the discrete analog of this conservation law to hold, the time integration method should satisfy a discrete analog of 2.21 and the discrete **curl** should satisfy a discrete analog of 2.24.

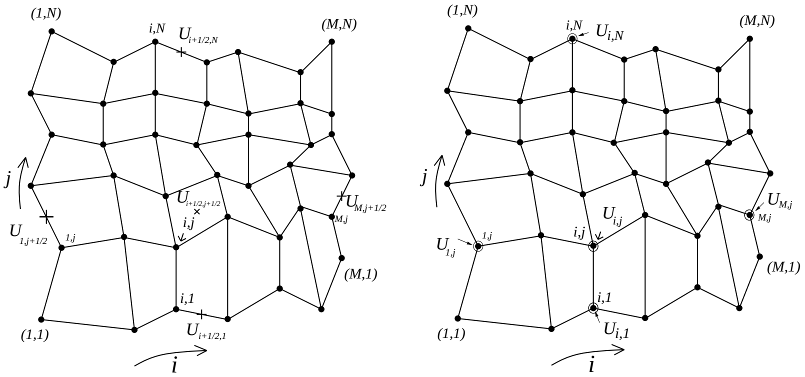

(a) Cell-centered grid, HC (b) Nodal grid, HN

FIG. 1. *On a logically rectangular grid, the scalar function values can be either cell-centered (HC), as in (a), or defined at the nodes (HN), as in (b).*

2.7. 2D-Case. We analyze the two dimensional case as a projection of the three dimensional case where there are no variations in the electromagnetic fields or geometry in the z direction. That is, all partial derivatives with respect to z are zero, and the domain extends to infinity in the z-direction with no change in the shape or position of its transverse cross section.

In this situation the full set of Maxwell's curl equations can presented as two groups of equations (see, for example ([52] pages 54-55)). The first group of equations involve only H_x, H_y and E_z, and are called the transverse magnetic (TM) mode equations. The second group of equations involve only E_x, E_y and H_z, and are called the transverse electric (TE) mode equations. The TM and TE modes are decoupled and can exist simultaneously with no mutual interaction. That is, they contain no common field vector components and are completely independent for structures composed of isotropic materials or anisotropic materials having no off-diagonal components in the constitutive tensors. These modes constitute the two possible ways that a electromagnetic field interaction problems can be two dimensional.

By preserving this decoupling in the discrete equations we prevent nonphysical interactions in discrete model.

3. Spaces of Discrete Functions.

3.1. Grid. We index the nodes of a logically rectangular grid using (i, j), where $1 \leq i \leq M$ and $1 \leq j \leq N$ (see Figure 1). The quadrilateral defined by the nodes (i, j), $(i + 1, j)$, $(i + 1, j + 1)$, and $(i, j + 1)$ is called the $(i + 1/2, j + 1/2)$ cell (see Figure 2 (a)). The area of the $(i + 1/2, j + 1/2)$ cell is denoted by $VC_{i+1/2,j+1/2}$, the length of the side that connects the vertices (i, j) and $(i, j+1)$ is denoted by $S\xi_{i,j+1/2}$, and the length of the side that connects the vertices (i, j) and $(i + 1, j)$ is denoted by $S\eta_{i+1/2,j}$. The angle between any two adjacent sides of cell (i, j) that meet at node (k, l) is denoted by $\varphi_{k,l}^{i+1/2,j+1/2}$.

When defining discrete differential operators, such as CURL, it is convenient to consider a 2-D grid as the projection of a 3-D grid. This approach simplifies the notation and later generalizing finite-difference methods to three dimensions. In this paper we consider functions of the coordinates x and y and extend the grid into a third dimension, z, by extending a grid line of unit length into the z direction to form

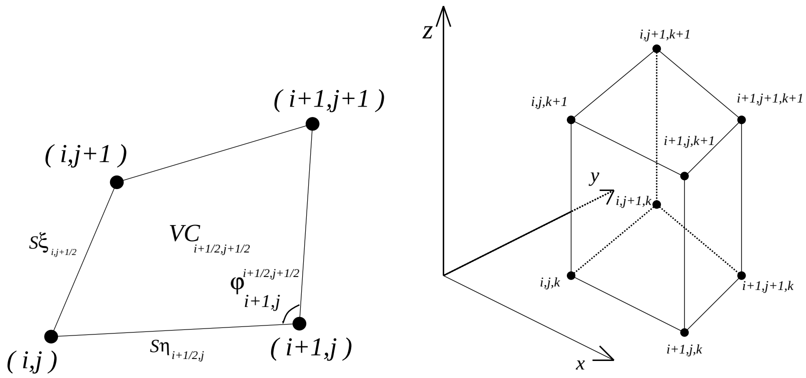

(a) 2-D grid (b) 3-D grid

FIG. 2. *(a) – The* $(i+1/2, j+1/2)$ *cell in a logically rectangular grid has area* $VC_{i+1/2,j+1/2}$ *and sides* $S\xi_{i,j+1/2}$, $S\eta_{i+1/2,j}$, $S\xi_{i+1,j+1/2}$, *and* $S\eta_{i+1/2,j+1}$. *The interior angle between* $S\eta_{i+1/2,j}$ *and* $S\xi_{i+1,j+1/2}$ *is* $\varphi_{i+1,j}^{i+1/2,j+1/2}$; *(b) – The 2-D* $(i+1/2, j+1/2)$ *cell* ($z=0$) *is interpreted as the base of a 3-D logically cuboid* $(i+1/2, j+1/2, k+1/2)$ *cell (a prism) with unit height.*

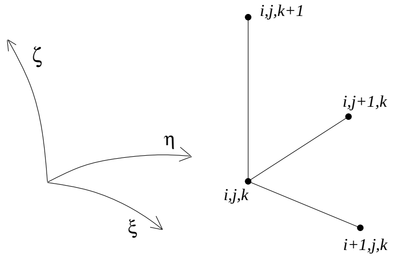

FIG. 3. *The* (ξ, η, ζ) *curvilinear coordinate system is approximated by the* $i, j,$ *and* k *piecewise linear grid lines.*

a prism with unit height and with a 2-D quadrilateral cell as its base (see Figure 2 (b)).

Sometimes it is useful to interpret the grid as being formed by intersections of broken lines that approximate the coordinate curves of some underlying curvilinear coordinate system (ξ, η, ζ). The ξ, η or ζ coordinate corresponds to the grid line where the index i, j or k is changing, respectively (see Figure 3).

We denote the length of the edge $(i,j,k)-(i+1,j,k)$ by $l\xi_{i+1/2,j,k}$, the length of the edge $(i,j,k)-(i,j+1,k)$ by $l\eta_{i,j+1/2,k}$, and the length of the edge $(i,j,k)-(i,j,k+1)$ by $l\zeta_{i,j,k+1/2}$ (which we have chosen to be equal to 1). The area of the surface $(i,j,k)-(i,j+1,k)-(i,j,k+1)-(i,j+1,k+1)$, denoted by $S\xi_{i,j+1/2,k+1/2}$, is the analog of the element of the coordinate surface $dS\xi$. Similarly, the area of surface $(i,j,k)-(i+1,j,k)-(i,j,k+1)-(i+1,j,k+1)$ is denoted by $S\eta_{i+1/2,j,k+1/2}$. We use the notation $S\zeta_{i+1/2,j+1/2,k}$ for the area of the 2-D cell $(i+1/2, j+1/2)$, that is, $S\zeta_{i+1/2,j+1/2,k} = VC_{i+1/2,j+1/2}$. Because the artificially constructed 3-D cell is a right prism with unit height, we have

$$S\xi_{i,j+1/2,k+1/2} = l\eta_{i,j+1/2,k} \cdot l\zeta_{i,j,k+1/2} = l\eta_{i,j+1/2,k}\,,$$

and

$$S\eta_{i+1/2,j,k+1/2} = l\xi_{i+1/2,j,k} \cdot l\zeta_{i,j,k+1/2} = l\xi_{i+1/2,j,k}\,.$$

With this 3-D interpretation, the 2-D notations $S\xi_{i,j+1/2}$ and $S\eta_{i+1/2,j}$ are not ambiguous because the 3-D surface $(i,j,k),(i,j+1,k),(i,j,k+1),(i,j+1,k+1)$ corresponds to an element of the coordinate surface $S\xi$ and, since the prism has unit height, the length of the side $(i,j)-(i,j+1)$ is equal to the area of the element of this coordinate surface.

3.2. Discrete Scalar and Vector Functions. In a cell-centered discretization, the discrete scalar function $U_{i+1/2,j+1/2}$ is defined in the space HC and is given by its values in the cells [see Figure 1 (a)], except at the boundary cells. The treatment of the boundary conditions requires introducing scalar function values at the centers of the boundary segments: $U_{(1,j+1/2)}$, $U_{(M,j+1/2)}$, where $j=1,\dots,N-1$, and $U_{(i+1/2,1)}$, $U_{(i+1/2,N)}$, where $i=1,\dots,M-1$. In three dimensions, the cell-centered scalar functions are defined in the centers of the 3-D prisms, except in the boundary cells where they are defined on the boundary faces. The 2-D case can be considered a projection of these values onto the 2-D cells and midpoints of the boundary segments. We will use cell-centered discretization for all scalar functions ϵ, μ and σ that determine material properties.

In a nodal discretization, the discrete scalar function $U_{i,j}$ is defined in the space HN and is given by its values in the nodes [see Figure 1 (b)]. The indices vary in the same range as for coordinates $x_{i,j}$, $y_{i,j}$.

We assume that vectors may have three components, but in our 2-D analysis, the components depend only on the two spatial coordinates, x and y. We consider two different spaces of discrete vector functions for our 3-D coordinate system. The $\mathcal{HS}$ space [see Figure 4 (a)], where the vector components are defined perpendicular to the cell faces, is the natural space when the approximations are based on Gauss' divergence theorem. The $\mathcal{HL}$ space [see Figure 5 (a)], where the vectors are defined tangential to the cell edges, is natural for approximations based on Stokes' circulation theorem.

The projection of the 3-D $\mathcal{HS}$ vector discretization space into two dimensions results in the face vectors being defined perpendicular to the quadrilateral cell sides and cell-centered vertical vector perpendicular to the 2-D plane [see Figure 4 (b)]. We use the notation

$$WS\xi_{(i,j+1/2)} \;: i=1,\dots,M\,;\; j=1,\dots,N-1$$

for the vector component at the center of face $S\xi_{(i,j+1/2)}$ (side $l\eta_{(i,j+1/2)}$), the notation

$$WS\eta_{(i+1/2,j)} \;: i=1,\dots,M-1\,;\; j=1,\dots,N$$

for the vector component at the center of face $S\eta_{(i+1/2,j)}$ (side $l\xi_{(i+1/2,j)}$), and the notation

$$WS\zeta_{(i+1/2,j+1/2)} \;: i=1,\dots,M-1\,;\; j=1,\dots,N-1$$

for the component at the center of face $S\zeta_{(i+1/2,j+1/2)}$ (2-D cell $V_{i+1/2,j+1/2}$).

The projection of the 3-D $\mathcal{HL}$ vector discretization space into two dimensions results in the vectors being defined as tangential to the quadrilateral cell sides and in a vertical vector at the nodes [see Figure 5 (b)]. We use the notation

$$WL\xi_{(i+1/2,j)} \;: i=1,\dots,M-1\,;\; j=1,\dots,N$$

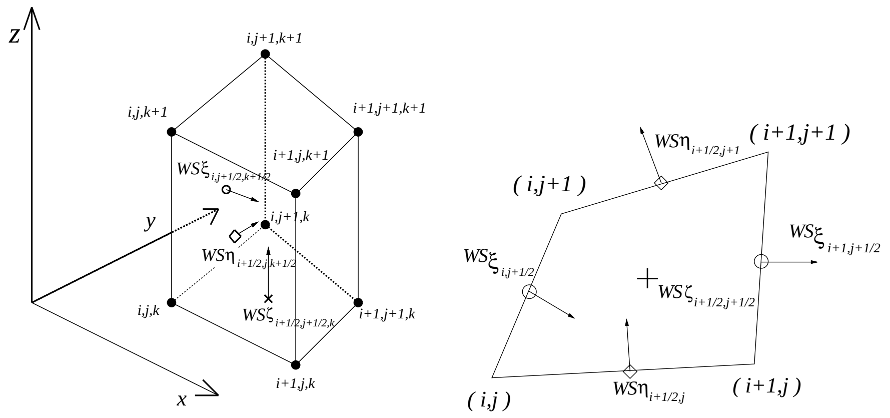

(a) $\mathcal{HS}$ in 3-D (b) $\mathcal{HS}$ in 2-D

FIG. 4. *(a) $\mathcal{HS}$ discretization of a vector in three dimensions; (b)* 2-D *interpretation of the $\mathcal{HS}$ discretization of a vector results in the face vectors being defined perpendicular to the cell sides and the vertical vectors being defined at cell centers perpendicular to the plane.*

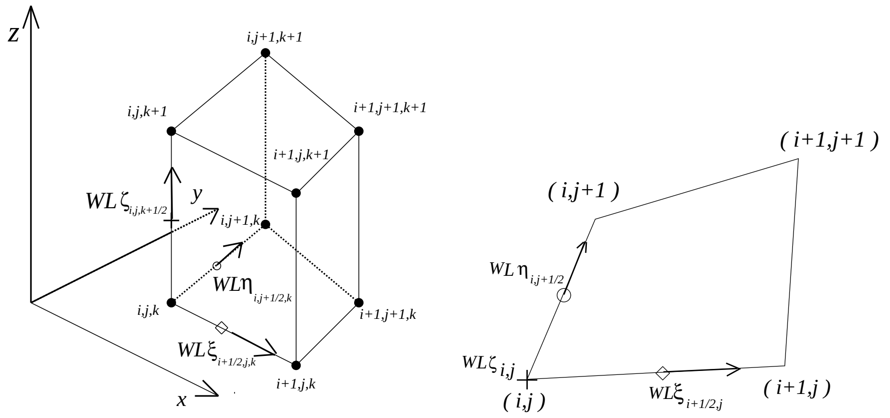

(a) $\mathcal{HL}$ in 3-D (b) $\mathcal{HL}$ in 2-D

FIG. 5. *(a) $\mathcal{HL}$ discretization of a vector in three dimensions; (b)* 2-D *interpretation of the $\mathcal{HL}$ discretization of a vector results in the edge vectors tangential to the cell sides and the vertical vectors being defined at cell nodes.*

for the component at the center of edge $l\xi_{(i+1/2,j)}$ [in 2-D, the same position as for $WS\eta_{(i+1/2,j)}$]; the notation

$$WL\eta_{(i,j+1/2)} \ : i = 1, \dots, M \, ; \, j = 1, \dots, N-1$$

for the component at the center of edge $l\eta_{(i,j+1/2)}$ [in 2-D, the same position as for $WS\xi_{(i,j+1/2)}$], and the notation

$$WL\zeta_{(i,j)} \ : i = 1, \dots, M \, ; \, j = 1, \dots, N$$

for the component at the center of edge $l\zeta_{(i,j)}$ [in 2-D the position that corresponds to node (i,j)].

From here on, there will not be any dependence on the k index, and it is dropped from the notations.

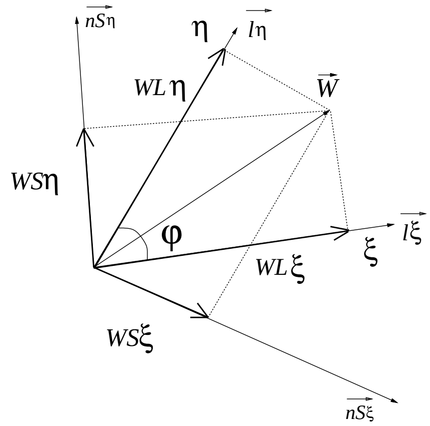

FIG. 6. *The grid lines* (ξ, η) *form a local nonorthogonal coordinate system with unit vectors* $\vec{l\xi}$, $\vec{l\eta}$ *and corresponding unit normals to these directions,* $n\vec{S}\xi$ *and* $n\vec{S}\eta$. *In this basis the components* $(WL\xi,\, WL\eta)$ *of vector* $\vec{W}$ *are the orthogonal projections onto the grid lines, and the components* $(WS\xi,\, WS\eta)$ *are the orthogonal projections to the normal directions.*

3.3. Discrete Inner Products. In the space of discrete scalar functions, HC, (functions defined in the cell centers), the *natural* inner product corresponding to the continuous inner product

$$(u, v)_H = \int_V u\, v\, dV + \oint_{\partial V} u\, v\, dV \tag{3.1}$$

is

$$\begin{aligned}(U, V)_{HC} = &\sum_{i=1}^{M-1} \sum_{j=1}^{N-1} U_{(i+1/2,j+1/2)}\, V_{(i+1/2,j+1/2)}\, VC_{(i+1/2,j+1/2)} \\ &+ \sum_{i=1}^{M-1} U_{(i+1/2,1)}\, V_{(i+1/2,1)}\, S\eta_{(i+1/2,1)} + \sum_{j=1}^{N-1} U_{(M,j+1/2)}\, V_{(M,j+1/2)}\, S\xi_{(M,j+1/2)} \\ &+ \sum_{i=1}^{M-1} U_{(i+1/2,N)}\, V_{(i+1/2,N)}\, S\eta_{(i+1/2,N)} \sum_{j=1}^{N-1} U_{(1,j+1/2)}\, V_{(1,j+1/2)}\, S\xi_{(1,j+1/2)}\,.\end{aligned}$$

We define $\overset{0}{HN}$ to be subspace of HN where discrete functions are equal to zero on the boundary

$$\overset{0}{HN} \overset{def}{=} \{U \in HN, U_{i,j} = 0 \text{ on the boundary}\}$$

(the notation of "zero" above the name of a space indicates the subspace where the functions are equal to zero on the boundary) with the inner product defined as

$$(U, V)_{\overset{0}{HN}} \overset{def}{=} \sum_{i=2}^{M-1} \sum_{j=2}^{N-1} U_{(i,j)}\, V_{(i,j)}\, VN_{(i,j)}\,, \tag{3.2}$$

where $VN_{(i,j)}$ is the nodal volume. From here on, we will use notation $\overset{def}{=}$, when we define a new object.

In the space of vector functions $\mathcal{HS}$, the *natural* inner product corresponding to the continuous inner product 4.14 is

$$(\vec{A},\vec{B})_{\mathcal{HS}} \stackrel{def}{=} \sum_{i=1}^{M-1}\sum_{j=1}^{N-1}(\vec{A},\vec{B})_{(i+1/2,j+1/2)}\,VC_{(i+1/2,j+1/2)}\,, \tag{3.3}$$

where $(\vec{A},\vec{B})$ is the dot product of two vectors. Next, we define this dot product in terms of the components of the vectors perpendicular to the cell sides (see Figure 6). Suppose that the axes ξ and η form a nonorthogonal basis and that φ is the angle between these axes. If the unit normals to the axes are $n\vec{S}\xi$ and $n\vec{S}\eta$, then the components of the vector $\vec{W}$ in this basis are the orthogonal projections $WS\xi$ and $WS\eta$ of $\vec{W}$ onto the normal vectors. The expression for the dot product of $\vec{A}=(AS\xi,AS\eta,AS\zeta)$ and $\vec{B}=(BS\xi,BS\eta,B\zeta)$, is

$$(\vec{A},\vec{B}) = \frac{AS\xi\,BS\xi + AS\eta\,BS\eta + (AS\xi\,BS\eta + AS\eta\,BS\xi)\,\cos\varphi}{\sin^2\varphi} + AS\zeta\,BS\zeta\,, \tag{3.4}$$

where φ is the angle between these axes (see Figure 6).

From this expression, the dot product in the cell is approximated by

$$\begin{aligned}(\vec{A},\vec{B})_{(i+1/2,j+1/2)} = {} & \sum_{k,l=0}^{1}\frac{V_{(i+k,j+l)}^{(i+1/2,j+1/2)}}{\sin^2\varphi_{(i+k,j+l)}^{(i+1/2,j+1/2)}} \\ & \cdot\Big[AS\xi_{(i+k,j+1/2)}\,BS\xi_{(i+k,j+1/2)} + AS\eta_{(i+1/2,j+l)}\,BS\eta_{(i+1/2,j+l)} \\ & +(-1)^{k+l}\,\Big(AS\xi_{(i+k,j+1/2)}\,BS\eta_{(i+1/2,j+l)} \\ & +\ AS\eta_{(i+1/2,j+l)}\,BS\xi_{(i+k,j+1/2)}\Big)\cos\varphi_{(i+k,j+l)}^{(i+1/2,j+1/2)}\Big] \\ & +AS\zeta_{i+1/2,j+1/2}\,BS\zeta_{i+1/2,j+1/2}\,,\end{aligned} \tag{3.5}$$

where the weights $V_{(i+k,j+l)}^{(i+1/2,j+1/2)}$ satisfy

$$V_{(i+k,j+l)}^{(i+1/2,j+1/2)} \geq 0\,, \quad \sum_{k,l=0}^{1} V_{(i+k,j+l)}^{(i+1/2,j+1/2)} = 1\,. \tag{3.6}$$

In this formula, each index (k,l) corresponds to one of the vertices of the $(i+1/2,j+1/2)$ cell, and notations for weights are the same as for angles of cell.

This dot product is the simplest robust approximation where if a cell angle is close to zero or π (and consequently the coordinate system related to this angle is close to degenerate), then the corresponding weight (and contribution from this vertex) vanishes smoothly when coordinate system became degenerate. Consequently, this dot product can be used for triangular cells that arise as the limit of degenerate quadrilaterals because the unknown component of the vector related to degenerate vertex does not appear in either the equation or the dot product.

This dot product can also be derived by averaging the dot products corresponding to piece-wise constant vector finite-elements (on each triangle). More accurate approximations for the dot product can be derived using the low-order Raviart-Thomas elements [43], [9] and includes terms like $AS\xi_{i,j+1/2}\cdot AS\xi_{i+1,j+1/2}$.

The inner product in $\mathcal{HL}$ is similar to the inner product for space $\mathcal{HS}$:

$$(\vec{A},\vec{B})_{\mathcal{HL}} \stackrel{def}{=} \sum_{i=1}^{M-1}\sum_{j=1}^{N-1}(\vec{A},\vec{B})_{(i+1/2,j+1/2)}\,VC_{(i+1/2,j+1/2)}\,, \tag{3.7}$$

where $(\vec{A},\vec{B})_{i+1/2,j+1/2}$ approximates the dot product of two vectors in the cell. In $\mathcal{HL}$, the vectors are represented by orthogonal projections to the directions of the edges of the 3-D cells (see Figure 6). If the axes ξ and η form a nonorthogonal basis, the components of the vector $\vec{W}$ in this basis are the orthogonal projections $WL\xi$ and $WL\eta$ of $\vec{W}$ onto the directions of the coordinate axes. If $\vec{A}=(AL\xi,AL\eta)$ and $\vec{B}=(BL\xi,BL\eta)$, then the dot product is

$$(\vec{A},\vec{B}) = \frac{AL\xi\,BL\xi + AL\eta\,BL\eta - (AL\xi\,BL\eta + AL\eta\,BL\xi)\,\cos\varphi}{\sin^2\varphi} + AL\zeta\,BL\zeta\,. \tag{3.8}$$

From a formal point of view, the only difference between this formula and the one for the surface components (see equation 3.4) is the minus sign before the third term. This difference can be easily understood by taking into account that the basis vectors of the nonorthogonal local systems are perpendicular to each other.

Equation 3.8 is used to approximate the dot product in a cell:

$$\begin{aligned}(\vec{A},\vec{B})_{(i+1/2,j+1/2)} = &\sum_{k,l=0}^{1}\frac{V_{(i+k,j+l)}^{(i+1/2,j+1/2)}}{\sin^2\varphi_{(i+k,j+l)}^{(i+1/2,j+1/2)}}\\ &\cdot\Big[AL\xi_{(i+1/2,j+l)}\,BL\xi_{(i+1/2,j+l)} + AL\eta_{(i+k,j+1/2)}\,BL\eta_{(i+k,j+1/2)}\\ &-(-1)^{k+l}\,\big(AL\xi_{(i+1/2,j+l)}\,BL\eta_{(i+k,j+1/2)}\\ &+\,AL\eta_{(i+k,j+1/2)}\,BL\xi_{(i+1/2,j+l)}\big)\cos\varphi_{(i+k,j+l)}^{(i+1/2,j+1/2)}\Big]\\ &+\sum_{k,l=0}^{1}V_{(i+k,j+l)}^{(i+1/2,j+1/2)}\,AL\zeta_{i+k,j+l}\,BL\zeta_{i+k,j+l}\,,\end{aligned} \tag{3.9}$$

where $V_{(i+k,j+l)}^{(i+1/2,j+1/2)}$ represents the same weights used for the space $\mathcal{HS}$.

When computing the adjoint relationships between the discrete operators, it is helpful to introduce the *formal* inner products, (denoted by square brackets $[\cdot,\cdot]$), in the spaces of scalar and vector functions. In HC, the formal inner product is

$$\begin{aligned}[U,V]_{HC} = &\sum_{i=1}^{M-1}\sum_{j=1}^{N-1}U_{(i+1/2,j+1/2)}\,V_{(i+1/2,j+1/2)} + \sum_{i=1}^{M-1}U_{(i+1/2,1)}\,V_{(i+1/2,1)}\\ &+\sum_{j=1}^{N-1}U_{(M,j+1/2)}\,V_{(M,j+1/2)} + \sum_{i=1}^{M-1}U_{(i+1/2,N)}\,V_{(i+1/2,N)} + \sum_{j=1}^{N-1}U_{(1,j+1/2)}\,V_{(1,j+1/2)}\,.\end{aligned}$$

In $\mathcal{HS}$, the formal inner product is

$$\begin{aligned}[\vec{A},\vec{B}]_{\mathcal{HS}} = &\sum_{i=1}^{M}\sum_{j=1}^{N-1}AS\xi_{(i,j+1/2)}\,BS\xi_{(i,j+1/2)} + \sum_{i=1}^{M-1}\sum_{j=1}^{N}AS\eta_{(i+1/2,j)}\,BS\eta_{(i+1/2,j)}\\ &+\sum_{i=1}^{M-1}\sum_{j=1}^{N-1}AS\zeta_{(i+1/2,j)}\,BS\zeta_{(i+1/2,j)}\,.\end{aligned}$$

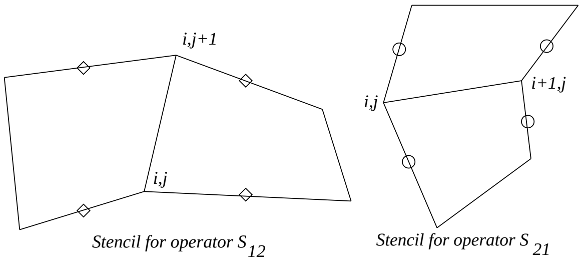

FIG. 7. *The stencils of the components S_{12} and S_{21} of the symmetric positive operator $\mathcal{S}$ that connects the natural and formal inner products $(\vec{A},\vec{B})_{\mathcal{HS}} = [\mathcal{S}\,\vec{A},\vec{B}]_{\mathcal{HS}}$.*

The natural and formal inner products satisfy the relationships

$$(U,V)_{HC} = [\mathcal{C}\,U,\,V]_{HC}\,, \quad \text{and} \quad (\vec{A},\vec{B})_{\mathcal{HS}} = [\mathcal{S}\,\vec{A},\,\vec{B}]_{\mathcal{HS}}\,, \tag{3.10}$$

where $\mathcal{C}$ and $\mathcal{S}$ are symmetric positive operators;

$$[\mathcal{C}\,U,V]_{HC} = [U,\mathcal{C}\,V]_{HC}\,, \quad \text{and} \quad [\mathcal{C}\,U,U]_{HC} > 0\,, \tag{3.11}$$

$$[\mathcal{S}\,\vec{A},\vec{B}]_{\mathcal{HS}} = [\vec{A},\mathcal{S}\,\vec{B}]_{\mathcal{HS}}\,, \quad [\mathcal{S}\,\vec{A},\vec{A}]_{\mathcal{HS}} > 0\,. \tag{3.12}$$

Therefore operator $\mathcal{C}$ satisfies the relations

$$\begin{aligned}
(\mathcal{C}\,U)_{(i+1/2,j+1/2)} &= VC_{(i+1/2,j+1/2)}\,U_{(i+1/2,j+1/2)}\,, \quad i=1,\cdots,M-1\,; \quad j=1,\cdots,N-1\,,\\
(\mathcal{C}\,U)_{(i,j+1/2)} &= S\xi_{(i,j+1/2)}\,U_{(i,j+1/2)}\,, \quad i=1 \text{ and } i=M\,; \quad j=1,\cdots,N-1\,,\\
(\mathcal{C}\,U)_{(i+1/2,j)} &= S\eta_{(i+1/2,j)}\,U_{(i+1/2,j)}\,, \quad i=1,\cdots,M-1\,; \quad j=1 \text{ and} j=N\,.
\end{aligned}$$

The operator $\mathcal{S}$ can be written in block form,

$$\mathcal{S}\,\vec{A} = \begin{pmatrix} S_{11} & S_{12} & 0 \\ S_{21} & S_{22} & 0 \\ 0 & 0 & S_{33} \end{pmatrix} \begin{pmatrix} AS\xi \\ AS\eta \\ AS\zeta \end{pmatrix} = \begin{pmatrix} S_{11}\,AS\xi + S_{12}\,AS\eta \\ S_{21}\,AS\xi + S_{22}\,AS\eta \\ S_{33}\,AS\zeta \end{pmatrix}. \tag{3.13}$$

By comparing the formal and natural inner products,

$$\begin{aligned}
(\vec{A},\vec{B})_{\mathcal{HS}} = [\mathcal{S}\,\vec{A},\vec{B}]_{\mathcal{HS}} &= \sum_{i=1}^{M}\sum_{j=1}^{N-1}[(S_{11}\,AS\xi)_{(i,j+1/2)} + (S_{12}\,AS\eta)_{(i,j+1/2)}]\,BS\xi_{(i,j+1/2)}\\
&+ \sum_{i=1}^{M-1}\sum_{j=1}^{N}[(S_{21}\,AS\xi)_{(i+1/2,j)} + (S_{22}\,AS\eta)_{(i+1/2,j)}]\,BS\eta_{(i+1/2,j)}\\
&\sum_{i=1}^{M-1}\sum_{j=1}^{N-1}(S_{33}\,AS\zeta)_{(i+1/2,j+1/2)}]\,BS\zeta_{(i+1/2,j+1/2)}\,,
\end{aligned} \tag{3.14}$$

we can derive the explicit formulas for $\mathcal{S}$:

$$(S_{11}\,AS\xi)_{(i,j+1/2)} = \left(\sum_{k=\pm\frac{1}{2};\,l=0,1} \frac{V_{(i,j+l)}^{(i+k,j+1/2)}}{\sin^2\varphi_{(i,j+l)}^{(i+k,j+1/2)}}\right) AS\xi_{(i,j+1/2)}\,,$$

$$(S_{12}\,AS\eta)_{(i,j+1/2)} = \sum_{k=\pm\frac{1}{2};l=0,1} (-1)^{k+\frac{1}{2}+l} \, \frac{V_{(i,j+l)}^{(i+k,j+1/2)}}{\sin^2\varphi_{(i,j+l)}^{(i+k,j+1/2)}} \, \cos\varphi_{(i,j+l)}^{(i+k,j+1/2)} \; AS\eta_{(i+k,j+l)}\,, \tag{3.15}$$

$$(S_{21}\,AS\xi)_{(i+1/2,j)} = \sum_{k=\pm\frac{1}{2};\,l=0,1} (-1)^{k+\frac{1}{2}+l} \, \frac{V_{(i+l,j)}^{(i+1/2,j+k)}}{\sin^2\varphi_{(i+l,j)}^{(i+1/2,j+k)}} \, \cos\varphi_{(i+l,j)}^{(i+1/2,j+k)} \, AS\xi_{(i+l,j+k)}\,,$$

$$(S_{22}\,AS\eta)_{(i+1/2,j)} = \left(\sum_{k=\pm\frac{1}{2};\,l=0,1} \frac{V_{(i+l,j)}^{(i+1/2,j+k)}}{\sin^2\varphi_{(i+l,j)}^{(i+1/2,j+k)}} \right) AS\eta_{(i+1/2,j)}\,,$$

$$(S_{33}\,AS\zeta)_{(i+1/2,j+1/2)} = V_{i+1/2,j+1/2}\,AS\zeta_{i+1/2,j+1/2}\,.$$

The operators S_{11}, S_{22} are diagonal, and the stencils for the operators S_{12} and S_{21} are shown on Figure 7. These formulas are valid only for sides of the grid cells interior to the domain. They can be applied at the sides on the domain boundary if the grid and discrete functions are first extended to a row of points outside the domain by using the appropriate boundary conditions.

The relationship between the natural and formal inner products in $\overset{0}{H}N$ is

$$(U,V)_{\overset{0}{H}N} = [\mathcal{N}\,U,\,V]_{\overset{0}{H}N}\,, \tag{3.16}$$

where $\mathcal{N}$ is a symmetric positive operator in the formal inner product,

$$[\mathcal{N}\,U,V]_{HN} = [U,\mathcal{N}\,V]_{HN}\,, \quad [\mathcal{N}\,U,U]_{HN} > 0\,, \tag{3.17}$$

and

$$(\mathcal{N}\,U)_{(i,j)} = VN_{(i,j)}\,U_{(i,j)}\,, \quad i = 2,\cdots,M-1\,; \quad j = 2,\cdots,N-1. \tag{3.18}$$

The operator $\mathcal{L}$, which connects the formal and natural inner products in $\mathcal{HL}$ (similar to operator $\mathcal{S}$ for space $\mathcal{HS}$) is symmetric and positive

$$(\vec{A},\,\vec{B})_{\mathcal{HL}} = [\mathcal{L}\,\vec{A},\vec{B}]_{\mathcal{HL}} = [\vec{A},\mathcal{L}\,\vec{B}]_{\mathcal{HL}}\,, \quad [\mathcal{L}\,\vec{A},\vec{A}]_{\mathcal{HL}} > 0\,, \tag{3.19}$$

and can be written in block form as

$$\mathcal{L}\,\vec{A} = \begin{pmatrix} L_{11} & L_{12} & 0 \\ L_{21} & L_{22} & 0 \\ 0 & 0 & L_{33} \end{pmatrix} \begin{pmatrix} AL\xi \\ AL\eta \\ AL\zeta \end{pmatrix} = \begin{pmatrix} L_{11}\,AL\xi + L_{12}\,AL\eta \\ L_{21}\,AL\xi + L_{22}\,AL\eta \\ L_{33}\,AL\zeta \end{pmatrix}. \tag{3.20}$$

A comparison of formal and natural inner products gives:

$$(L_{11}\,AL\xi)_{(i+1/2,j)} = \left(\sum_{k=\pm\frac{1}{2};\,l=0,1} \frac{V_{(i+l,j)}^{(i+1/2,j+k)}}{\sin^2\varphi_{(i,j+l)}^{(i+1/2,j+k)}} \right) AL\xi_{(i+1/2,j)}\,,$$

$$(L_{12}\,AL\eta)_{(i+1/2,j)} = -\sum_{k=\pm\frac{1}{2};\,l=0,1} (-1)^{k+\frac{1}{2}+l} \, \frac{V_{(i+l,j)}^{(i+1/2,j+k)}}{\sin^2\varphi_{(i+l,j)}^{(i+1/2,j+k)}} \, \cos\varphi_{(i+l,j)}^{(i+1/2,j+k)} \; AL\eta_{(i+l,j+k)}\,, \tag{3.21}$$

$$(L_{21}\,AL\xi)_{(i,j+1/2)} = -\sum_{k=\pm\frac{1}{2};\,l=0,1} (-1)^{k+\frac{1}{2}+l}\,\frac{V_{(i,j+l)}^{(i+k,j+1/2)}}{\sin^2\varphi_{(i,j+l)}^{(i+k,j+1/2)}}\,\cos\varphi_{(i,j+l)}^{(i+k,j+1/2)}\,AL\xi_{(i+k,j+l)}\,,$$

$$(L_{22}\,AL\eta)_{(i,j+1/2)} = \left(\sum_{k=\pm\frac{1}{2};\,l=0,1} \frac{V_{(i,j+l)}^{(i+k,j+1/2)}}{\sin^2\varphi_{(i,j+l)}^{(i+k,j+1/2)}}\right) AL\eta_{(i,j+1/2)}\,,$$

$$(L_{33}\,AL\zeta)_{(i,j)} = \left(\sum_{k=\pm\frac{1}{2};\,l=\pm\frac{1}{2}} V_{(i,j)}^{(i+k,j+l)}\right) AL\zeta_{(i,j)}\,.$$

The operators L_{11} and L_{22} are diagonal, and the stencils for the operators L_{21} and L_{12} (in 2-D) are the same as for the operators S_{12} and S_{21} (see Figure 7).

These discrete inner products satisfy the axioms of inner products, that is,

- $(A,\,B)_{H_h} = (B,\,A)_{H_h}$,
- $(\lambda\,A,\,B)_{H_h} = \lambda\,(A,\,B)_{H_h}$, (for all real numbers λ)
- $(A_1 + A_2,\,B)_{H_h} = (A_1\,B)_{H_h} + (A_2\,B)_{H_h}$,
- $(A,\,A)_{H_h} \geq 0$ and $(A,\,A)_{H_h} = 0$ if and only if $A = 0$.

In these axioms A and B are either discrete scalar or discrete vector functions and $(\cdot,\cdot)_{H_h}$ is the appropriate discrete inner product.

Therefore the discrete inner products are true inner products and not just approximations of the continuous inner products. Also, discrete spaces are Euclidean spaces.

4. Discrete Analogs of div, grad, and curl.

4.1. Natural Operators.

4.1.1. Natural Operator DIV**.** The coordinate invariant definition of the **div** operator is based on Gauss' divergence theorem:

$$\mathbf{div}\,\vec{W} = \lim_{V\to 0} \frac{\oint_{\partial V} (\vec{W},\vec{n})\,dS}{V}\,, \tag{4.1}$$

where $\vec{n}$ is a unit outward normal to boundary ∂V. To extend the operator **div** to the boundary, we define the extended divergence operator $\mathbf{d}$ as

$$\mathbf{d}\vec{w} = \begin{cases} +\mathbf{div}\,\vec{w}\,, & (x,y) \in V \\ -(\vec{w},\vec{n})\,, & (x,y) \in \partial V \end{cases}. \tag{4.2}$$

The corresponding natural definition of the discrete divergence operator is

$$\mathrm{DIV} : \mathcal{HS} \to HC\,, \tag{4.3}$$

where

$$\begin{aligned}&(\mathrm{DIV}\,\vec{W})_{(i+1/2,j+1/2)} = \\ &\frac{1}{VC_{(i,j)}}\,\big\{\big(WS\xi_{(i+1,j+1/2)}\,S\xi_{(i+1,j+1/2)} - WS\xi_{(i,j+1/2)}\,S\xi_{(i,j+1/2)}\big) + \\ &\big(WS\eta_{(i+1/2,j+1)}\,S\eta_{(i+1/2,j+1)} - WS\eta_{(i+1/2,j)}\,S\eta_{(i+1/2,j)}\big)\big\}\,.\end{aligned} \tag{4.4}$$

The discrete extended divergence $\mathbf{D}$ coincides with DIV, $(\mathbf{D}\,\vec{W})_{(i+1/2,j+1/2)} = (\mathrm{DIV}\,\vec{W})_{(i+1/2,j+1/2)}$ on the internal cells and is defined on the boundary by

$$(\mathbf{D}\,\vec{W})_{(i+1/2,1)} = -WS\eta_{(i+1/2,1)}\,, \quad i = 1,\cdots,M-1\,,$$

$$(\mathbf{D}\,\vec{W})_{(i+1/2,N)} = +WS\eta_{(i+1/2,N)}\,, \quad i = 1, \cdots, M-1\,, \tag{4.5}$$
$$(\mathbf{D}\,\vec{W})_{(1,j+1/2)} = -WS\xi_{(1,j+1/2)}\,, \quad j = 1, \cdots, N-1\,,$$
$$(\mathbf{D}\,\vec{W})_{(M,j+1/2)} = +WS\xi_{(M,j+1/2)}\,, \quad j = 1, \cdots, N-1\,.$$

4.1.2. Natural Operator GRAD. For any direction l given by the unit vector $\vec{l}$, the directional derivative can be defined as

$$\frac{\partial u}{\partial l} = (\mathbf{grad}\, u, \vec{l})\,. \tag{4.6}$$

For a function $U_{i,j} \in HN$, this relationship leads to the coordinate invariant definition of the natural discrete gradient operator:

$$\mathrm{GRAD} : HN \to \mathcal{HL}\,. \tag{4.7}$$

The vector $\vec{G} = \mathrm{GRAD}\, U$ is defined as

$$GL\xi_{i+1/2,j} = \frac{U_{i+1,j} - U_{i,j}}{l\xi_{i+1/2,j}}\,,\ GL\eta_{i,j+1/2} = \frac{U_{i,j+1} - U_{i,j}}{l\eta_{i,j+1/2}}\,,\ GL\zeta_{i,j} = 0\,. \tag{4.8}$$

Note that if $\mathrm{GRAD}\, U = 0$, then the scalar discrete function U is a constant, and vice versa.

4.1.3. Natural Operator CURL. The coordinate invariant definition of the **curl** operator is based on Stoke's circulation theorem,

$$(\vec{n}, \mathbf{curl}\, \vec{B}) = \lim_{S \to 0} \frac{\oint_l (\vec{B}, \vec{l})\, dl}{S}\,, \tag{4.9}$$

where S is the surface spanning (based on) the closed curve l, $\vec{n}$ is the unit outward normal to S, and $\vec{l}$ is the unit tangential vector to t As we already noted in Introduction using this definition to define discrete curl will guarantee that law of electromagnetic induction will be preserved in discrete case for each face of the cell.

Using the discrete analog of equation 4.9, we can obtain expressions for components of vector $\vec{R} = (RS\xi, RS\eta, RS\zeta) = \mathrm{CURL}\, \vec{B}$, where the discrete natural curl

$$\mathrm{CURL} : \mathcal{HL} \to \mathcal{HS},$$

and

$$RS\xi_{i,j+1/2} = \tag{4.10-a}$$
$$\frac{BL\zeta_{i,j+1}\, l\zeta_{i,j+1,k+1/2} - BL\zeta_{i,j}\, l\zeta_{i,j,k+1/2}}{S\xi_{i,j+1/2,k+1/2}} =$$
$$\frac{BL\zeta_{i,j+1} - BL\zeta_{i,j}}{l\eta_{i,j+1/2}}\,,$$
$$RS\eta_{i+1/2,j} = \tag{4.10-b}$$
$$-\frac{BL\zeta_{i+1,j,k+1/2}\, l\zeta_{i+1,j,k+1/2} - BL\zeta_{i,j,k+1/2}\, l\zeta_{i,j,k+1/2}}{S\eta_{i+1/2,j,k+1/2}} =$$
$$-\frac{BL\zeta_{i+1,j} - BL\zeta_{i,j}}{l\xi_{i+1/2,j}}\,,$$
$$RS\zeta_{i+1/2,j+1/2} = \tag{4.10-c}$$
$$\{ \left(BL\eta_{i+1,j+1/2}\, l\eta_{i+1,j+1/2} - BL\eta_{i,j+1/2}\, l\eta_{i,j+1/2}\right) -$$
$$\{ \left(BL\xi_{i+1/2,j+1}\, l\xi_{i+1/2,j+1} - BL\xi_{i+1/2,j}\, l\xi_{i+1/2,j}\right) \} / \, S\zeta_{i+1/2,j+1/2}\,,$$

(see [21] for details).

Note that if $\vec{B} = (0, 0, BL\zeta)$, then the condition $\mathrm{CURL}\,\vec{B} = 0$ is equivalent to $BL\zeta_{i,j} = const$.

The expressions for $RS\xi$ and $RS\eta$ contain only the $BL\zeta$ component of $\vec{B}$ and the expression for $RS\zeta$ contains only the $BL\xi$ and $BL\eta$ components. This fact will allow us to introduce discrete analogs of the TM and TE modes.

The operator CURL can be presented in (3×3) block form

$$\mathrm{CURL} = \begin{pmatrix} 0 & 0 & R_{13} \\ 0 & 0 & R_{23} \\ R_{31} & R_{23} & 0 \end{pmatrix}, \tag{4.11}$$

where

$$\begin{aligned}
(R_{13}\,BL\zeta)_{i,j+1/2} &= \frac{BL\zeta_{i,j+1} - BL\zeta_{i,j}}{l\eta_{i,j+1/2}} \\
(R_{23}\,BL\zeta)_{i+1/2,j} &= -\frac{BL\zeta_{i+1,j} - BL\zeta_{i,j}}{l\xi_{i+1/2,j}} \\
(R_{31}\,BL\xi)_{i+1/2,j+1/2} &= -\frac{BL\xi_{i+1/2,j+1}\,l\xi_{i+1/2,j+1} - BL\xi_{i+1/2,j}\,l\xi_{i+1/2,j}}{S\zeta_{i+1/2,j+1/2}}, \\
(R_{32}\,BL\eta)_{i+1/2,j+1/2} &= \frac{BL\eta_{i+1,j+1/2}\,l\eta_{i+1,j+1/2} - BL\eta_{i,j+1/2}\,l\eta_{i,j+1/2}}{S\zeta_{i+1/2,j+1/2}}.
\end{aligned} \tag{4.12}$$

This structure of the CURL will be used to derive the discrete adjoint operator $\overline{\mathrm{CURL}}$.

4.1.4. Properties of Natural Discrete Operators. The natural discrete operators satisfy discrete analogs of the theorems of vector analysis [21] including Gauss' theorem; the theorem that $\mathbf{div}\,\vec{A} = 0$ if and only if $\vec{A} = \mathbf{curl}\,\vec{B}$; $\mathbf{curl}\,\vec{A} = 0$ if and only if $\vec{A} = \mathbf{grad}\varphi$; the theorem that if $\vec{A} = \mathbf{grad}\,\varphi$, then the line integral does not depend on path; and the theorem that if the line integral of a vector function is equal to zero for any closed path, then this vector is the gradient of a scalar function.

In this paper we use two theorems:

$\mathrm{DIV}\vec{A} = 0$ if and only if $\vec{A} = \mathrm{CURL}\,\vec{B}$, where $\vec{A} \in \mathcal{HS}$ and $\vec{B} \in \mathcal{HL}$;

$\mathrm{CURL}\,\vec{A} = 0$ if and only if $\vec{A} = \mathrm{GRAD}\,U$, where $\vec{A} \in \mathcal{HL}$ and $U \in HN$.

4.2. Adjoint Operators. In [22] we use the SOM to derive the operators $\overline{\mathrm{DIV}}$, $\overline{\mathrm{GRAD}}$, and $\overline{\mathrm{CURL}}$ from discrete analogs of the integral identities 1.9 and 1.5 These identities connect the differential operators **div**, **grad**, and **curl** and allow us to obtain their discrete analogs with consistent domains and ranges of values.

4.2.1. Operator $\overline{\mathrm{GRAD}}$. To construct the operator $\overline{\mathrm{GRAD}}$ we use a discrete analog of the identity 1.9. If we introduce the space of scalar functions H with the inner product

$$(u,\,v)_H = \int_V u\,v\,dV + \oint_{\partial V} u\,v\,dS\,, \quad u, v \in H\,, \tag{4.13}$$

and the space of vector functions $\mathbf{H}$ with inner product defined as

$$(\vec{A},\,\vec{B})_{\mathbf{H}} = \int_V (\vec{A},\,\vec{B})\,dV\,, \quad \vec{A}, \vec{B} \in \mathbf{H}\,, \tag{4.14}$$

then the identity 1.9 implies

$$\mathbf{d} = -\mathbf{grad}^* , \tag{4.15}$$

or

$$\begin{aligned}(\mathbf{d}\,\vec{w},\, u)_H &= \int_V u\,\mathbf{div}\,\vec{w}\,dV - \oint_{\partial V} u\,(\vec{w},\,\vec{n})\,dS \\ &= -\int_V (\vec{w},\,\mathbf{grad} u)\,dV \\ &= (\vec{w},\,-\mathbf{grad}\,u)_{\mathbf{H}} .\end{aligned} \tag{4.16}$$

We base the definition of $\overline{\mathrm{GRAD}}$ on a discrete analog of 4.15. In section 4.1.1 we defined the operator $\mathbf{D}$ as the discrete analog of the continuous operator $\mathbf{d}$. Therefore, the derived gradient operator is defined by $\overline{\mathrm{GRAD}} \stackrel{def}{=} -\mathbf{D}^*$, where the adjoint is taken in the natural inner products.

Because $\mathbf{D} : \mathcal{HS} \to HC$, the adjoint operator is defined in terms of the inner products

$$(\mathbf{D}\,\vec{W}, U)_{HC} = (\vec{W}, \mathbf{D}^* U)_{\mathcal{HS}} , \tag{4.17}$$

which can be translated into the formal inner products as

$$[\mathbf{D}\,\vec{W}, \mathcal{C}\,U]_{HC} = [\vec{W}, \mathcal{S}\,\mathbf{D}^* U]_{\mathcal{HS}} . \tag{4.18}$$

The formal adjoint $\mathbf{D}^\dagger$ of $\mathbf{D}$ is defined to be the adjoint in the formal inner product

$$[\vec{W}, \mathbf{D}^\dagger\,\mathcal{C}\,U]_{\mathcal{HS}} = [\vec{W}, \mathcal{S}\,\mathbf{D}^* U]_{\mathcal{HS}} . \tag{4.19}$$

This relationship must be true for all $\vec{W}$ and U. Therefore $\mathbf{D}^\dagger\,\mathcal{C} = \mathcal{S}\,\mathbf{D}^*$ or $\mathbf{D}^* = \mathcal{S}^{-1}\,\mathbf{D}^\dagger\,\mathcal{C}$, and the discrete analog of the operator **grad** can be represented as

$$\overline{\mathrm{GRAD}} = -\mathbf{D}^* = -\mathcal{S}^{-1}\,\mathbf{D}^\dagger\,\mathcal{C} . \tag{4.20}$$

Because the operator $\mathcal{S}$ is banded on nonorthogonal grids, its inverse $\mathcal{S}^{-1}$ is full, and it is not possible to derive explicit formulas for the components of the operator $\overline{\mathrm{GRAD}}$. Consequently, $\overline{\mathrm{GRAD}}$ has a *nonlocal* stencil.

The discrete flux,

$$\vec{W} = -\overline{\mathrm{GRAD}}\,U = \mathcal{S}^{-1}\,\mathbf{D}^\dagger\,\mathcal{C}\,U ,$$

is obtained by solving the banded linear system (recall that $\mathcal{C}$, $\mathcal{S}$, and $\mathbf{D}$ are local operators)

$$\mathcal{S}\,\vec{W} = \mathbf{D}^\dagger\,\mathcal{C}\,U , \tag{4.21}$$

where the right-hand side, $F = (FS\xi,\, FS\eta) = \mathbf{D}^\dagger\,\mathcal{C}\,U$, is

$$\begin{aligned}FS\xi_{i,j+1/2} &= -S\xi_{i,j+1/2}\,(U_{i+1/2,j+1/2} - U_{i-1/2,j+1/2}) \\ FS\eta_{i+1/2,j} &= -S\eta_{i+1/2,j}\,(U_{i+1/2,j+1/2} - U_{i+1/2,j-1/2})\end{aligned} \tag{4.22}$$

The discrete operator $\mathcal{S}$ is a symmetric positive definite and can be represented as matrix with five nonzero elements in each row (see, equation 3.15 and Figure 7).

To prove that $\overline{\text{GRAD}}\,U$ is zero if and only if U is constant, note that equation 4.22 implies that if U is a constant, then $\mathcal{D}^{\dagger}\,\mathcal{M}\,U = 0$ and therefore $\overline{\text{GRAD}}\,U = \mathcal{S}^{-1}\,\mathcal{D}^{\dagger}\,\mathcal{M}\,U = 0$. Conversely, if we assume $\overline{\text{GRAD}}\,U = 0$, then equation 4.20 and the fact that $\mathcal{S}$ is positive definite implies

$$\mathcal{D}^{\dagger}\,\mathcal{M}\,U = 0\,. \tag{4.23}$$

This and equation 4.22 then give:

$$\begin{aligned} &U_{(i+1/2,j+1/2)} - U_{(i-1/2,j+1/2)} = 0\,; \quad i = 1,\ldots,M\,; \quad j = 1,\ldots,N-1\,; \\ &U_{(i+1/2,j+1/2)} - U_{(i+1/2,j-1/2)} = 0\,; \quad i = 1,\ldots,M-1\,; \quad j = 1,\ldots,N\,; \end{aligned}$$

which implies that U is a constant. Therefore the null space of the discrete operator $\overline{\text{GRAD}}$ is composed only of the constant functions.

4.2.2. Operators $\overline{\text{DIV}}$ and $\overline{\text{DIV}}^{\epsilon}$. The operator $\overline{\text{DIV}}$ is defined as the negative adjoint to the natural operator GRAD. In the subspace of scalar functions, $\overset{0}{H}$, where $u(x,y) = 0\,,(x,y) \in \partial V$, the boundary term in integral identity 1.9 is zero, and therefore

$$\int_V (\vec{W}, \mathbf{grad}\; u)\, dV = -\int_V u\, \mathbf{div}\, \vec{W}\, dV\,. \tag{4.24}$$

That is, in this subspace **div** is the negative adjoint of **grad**:

$$(u,v)_{\overset{0}{H}} = \int_V u\,v\,dV\,, \quad \text{and} \quad (\vec{A},\vec{B})_{\mathcal{H}} = \int_V (\vec{A},\vec{B})\,dV\,. \tag{4.25}$$

The discrete adjoint operator $\overline{\text{DIV}} : \mathcal{HL} \to \overset{0}{H}N$ is defined as the negative adjoint of the discrete natural operator GRAD $:\overset{0}{H}N \to \mathcal{HL}$,

$$\overline{\text{DIV}} \overset{def}{=} -\text{GRAD}^{*}\,. \tag{4.26}$$

Using the connections between the formal and natural inner products,

$$\overline{\text{DIV}} = -\mathcal{N}^{-1} \cdot \text{GRAD}^{\dagger} \cdot \mathcal{L}\,. \tag{4.27}$$

$\overline{\text{DIV}}$ is local because $\mathcal{N}$ is diagonal, and both $\text{GRAD}^{\dagger}$ and $\mathcal{L}$ are local. It is easy to see that

$$-\text{GRAD}^{\dagger}\,\vec{A} = \left(\frac{AL\xi_{i+1/2,j}}{l\xi_{i+1/2,j}} - \frac{AL\xi_{i-1/2,j}}{l\xi_{i-1/2,j}}\right) + \left(\frac{AL\eta_{i,j+1/2}}{l\eta_{i,j+1/2}} - \frac{AL\eta_{i,j-1/2}}{l\eta_{i,j-1/2}}\right)\,.$$

The stencil for $\overline{\text{DIV}}$ at the interior nodes (shown in Figure 8) is obtained by combining this formula with the stencil for operators L_{11}, L_{12}, L_{21}, and L_{22} defined in 3.21.

The operator $\overline{\text{DIV}}^{\epsilon}$ is the discrete analog of $\mathbf{div}^{\epsilon} \overset{def}{=} \mathbf{div} \cdot \epsilon$, which applies the tensor ϵ and then **div**. On nonsmooth, nonorthogonal grid, or when ϵ is discontinuous it is not possible to separate these two operations on discrete level. We need discrete analog of operator $\mathbf{div}^{\epsilon}$ because our primary variable for the electric field is $\vec{E}$, and

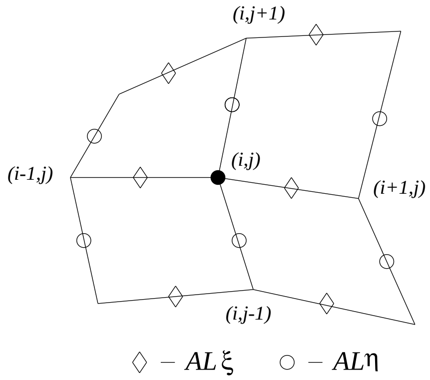

FIG. 8. *Stencil for the operator* $\overline{\mathrm{DIV}} = -\mathrm{GRAD}^* : \mathcal{HL} \to \overset{0}{HN}$.

we want to satisfy a discrete analog of Gauss's law $\mathbf{div}\,\vec{D} = \mathbf{div}^\epsilon\,\vec{E} = \rho$. The domain of $\overline{\mathrm{DIV}}^\epsilon$ is $\mathcal{HL}$ and range of values is HN. Therefore, the ρ is defined at the nodes HN, and the discrete Gauss's law will be valid at the nodes.

To define $\overline{\mathrm{DIV}}^\epsilon$ we modify the identity 4.24 by changing $\vec{W}$ to $\epsilon\,\vec{W}$

$$\int_V \epsilon(\vec{W}, \mathbf{grad}\; u)\, dV = -\int_V u\, \mathbf{div}^\epsilon\, \vec{W}\, dV\,. \tag{4.28}$$

That is, operator $\mathbf{div}^\epsilon$ is the negative adjoint to $\mathbf{grad}$ in the inner product

$$(\vec{A}, \vec{B})^\epsilon_{\mathcal{H}} \stackrel{def}{=} \int_V \epsilon\,(\vec{A}, \vec{B})\, dV\,. \tag{4.29}$$

To derive the compatible operator $\overline{\mathrm{DIV}}^\epsilon$ we must define a similar inner product $(\cdot,\,\cdot)^\epsilon_{\mathcal{HL}}$ in the discrete space $\mathcal{HL}$ from standard one $(\cdot,\,\cdot)_{\mathcal{HL}}$ by multiplying $V^{i+1/2,j+1/2}_{i+k,j+l}$ by $\epsilon_{i+1/2,j+1/2}$. This leads to a modified $\mathcal{L}$ operator, $\mathcal{L}^\epsilon$, and $\overline{\mathrm{DIV}^\epsilon}$ is defined by

$$\overline{\mathrm{DIV}^\epsilon} = -\mathcal{N}^{-1} \cdot \mathrm{GRAD}^\dagger \cdot \mathcal{L}^\epsilon\,. \tag{4.30}$$

4.2.3. Operators $\overline{\mathrm{CURL}}$ and ${}_\epsilon\overline{\mathrm{CURL}}_\mu$. In the subspace of vectors $\vec{A}$, where the surface integral in 1.5 on the right-hand side vanishes, we have

$$\int_V (\mathbf{curl}\vec{A}, \vec{B})\, dV = \int_V (\vec{A}, \mathbf{curl}\,\vec{B})\, dV\,. \tag{4.31}$$

That is, in this subspace of vector functions, $\mathbf{curl}$ is self-adjoint, $\mathbf{curl} = \mathbf{curl}^*$, in the $\mathcal{H}$ inner product $(\vec{A}, \vec{B})_{\mathcal{H}}$.

We define the discrete adjoint operator $\overline{\mathrm{CURL}} : \mathcal{HS} \to \mathcal{HL}$ as the adjoint to the discrete natural operator $\mathrm{CURL} : \mathcal{HL} \to \mathcal{HS}$ by

$$\overline{\mathrm{CURL}} \stackrel{def}{=} \mathrm{CURL}^*\,. \tag{4.32}$$

That is,

$$(\mathrm{CURL}\,\vec{A}, \vec{B})_{\mathcal{HS}} = (\vec{A}, \overline{\mathrm{CURL}}\,\vec{B})_{\mathcal{HL}}\,, \tag{4.33}$$

and $\overline{\mathrm{CURL}}$ can be expressed as

$$\overline{\mathrm{CURL}} = \mathcal{L}^{-1} \cdot \mathrm{CURL}^{\dagger} \cdot \mathcal{S} \,. \tag{4.34}$$

Although CURL is a local operator, the operator $\overline{\mathrm{CURL}}$ is *nonlocal*. We can determine $\vec{\mathbf{C}} = \overline{\mathrm{CURL}}\,\vec{B}$ by solving the system of linear equations

$$\mathcal{L}\,\vec{\mathbf{C}} = \mathrm{CURL}^{\dagger} \cdot \mathcal{S}\,\vec{B} \,, \tag{4.35}$$

with local operators $\mathcal{L}$ and $\mathrm{CURL}^{\dagger} \cdot \mathcal{S}$.

Using equation 4.12 note

$$\overline{\mathrm{CURL}} = \begin{pmatrix} 0 & 0 & R^{\dagger}_{31} \\ 0 & 0 & R^{\dagger}_{32} \\ R^{\dagger}_{13} & R^{\dagger}_{32} & 0 \end{pmatrix} , \tag{4.36}$$

where

$$\begin{aligned}
\left(R^{\dagger}_{31}\, AS\zeta\right)_{i+1/2,j} &= -l\xi_{i+1/2,j}\left(\frac{AS\zeta_{i+1/2,j-1/2}}{S\zeta_{i+1/2,j-1/2}} - \frac{AS\zeta_{i+1/2,j+1/2}}{S\zeta_{i+1/2,j+1/2}}\right) \\
\left(R^{\dagger}_{32}\, AS\zeta\right)_{i,j+1/2} &= l\eta_{i,j+1/2}\left(\frac{AS\zeta_{i-1/2,j+1/2}}{S\zeta_{i-1/2,j+1/2}} - \frac{AS\zeta_{i+1/2,j+1/2}}{S\zeta_{i+1/2,j+1/2}}\right) \\
\left(R^{\dagger}_{13}\, AS\xi\right)_{i,j} &= \left(\frac{AS\xi_{i,j-1/2}}{l\eta_{i,j-1/2}} - \frac{AS\xi_{i,j+1/2}}{l\eta_{i,j+1/2}}\right) \\
\left(R^{\dagger}_{23}\, AS\eta\right)_{i,j} &= -\left(\frac{AS\eta_{i-1/2,j}}{l\xi_{i-1/2,j}} - \frac{AS\eta_{i+1/2,j}}{l\xi_{i+1/2,j}}\right) .
\end{aligned}$$

It easy to prove that $\overline{\mathrm{CURL}}\,\vec{B} = 0$ implies that $BS\zeta_{i,j} = const.$ when $\vec{B} = (0,\, 0,\, BS\zeta)$.

Also using the structure of operators $\mathcal{S}$, $\mathcal{L}$ and $\mathrm{CURL}^{\dagger}$ we can write equation 4.35 for finding components of $\overline{\mathrm{CURL}}$ as

$$\begin{aligned}
& L_{11}\, CL\xi + L_{12}\, CL\eta = R^{\dagger}_{31}\, S_{33}\, BS\zeta \,, \\
& L_{21}\, CL\xi + L_{22}\, CL\eta = R^{\dagger}_{32}\, S_{33}\, BS\zeta \,, \\
& L_{33}\, CL\zeta = R^{\dagger}_{13}\, \left(S_{11}\, BS\xi + S_{12}\, BS\eta\right) + R^{\dagger}_{23}\, \left(S_{21}\, BS\xi + S_{22}\, BS\eta\right) = \\
& \left(R\,\dagger_{13} \cdot S_{11} + R^{\dagger}_{23} \cdot S_{21}\right)\, BS\xi + \left(R\,\dagger_{13} \cdot S_{12} + R^{\dagger}_{23} \cdot S_{22}\right)\, BS\eta \,.
\end{aligned}$$

The first two equations can be decoupled from third. Consequently, we also can separate the TM and TE modes for $\overline{\mathrm{CURL}}$.

Because of our choice of primary variables for solving equation 2.12-b, we must derive a discrete approximation for the compound operator ${}_{\epsilon}\mathbf{curl}_{\mu} \overset{def}{=} \frac{1}{\epsilon}\,\mathbf{curl}\,\frac{1}{\mu}$. Again as for $\mathbf{div}^{\epsilon}$, if ϵ and μ are discontinuous it is not possible to separate them from the **curl** in the discrete approximation. We will define the discrete analog of ${}_{\epsilon}\mathbf{curl}_{\mu}$ after introducing new inner products for both discrete spaces. Modifying the identity for curls we have

$$\int_V \frac{1}{\mu}\,(\mathbf{curl}\vec{A}, \vec{B})\, dV = \int_V \epsilon(\vec{A}, \frac{1}{\epsilon}\,\mathbf{curl}\,\frac{\vec{B}}{\mu})\, dV \,. \tag{4.37}$$

The modified inner product in $\mathcal{HS}$, $(\cdot,\,\cdot)^{\frac{1}{\mu}}_{\mathcal{HS}}$, uses the weight $1/\mu$ and the inner product in the space $\mathcal{HL}$ uses the weight ϵ, as we did when defining DIV^ϵ. The compound discrete adjoint curl is defined as

$$ {}_\epsilon\overline{\mathrm{CURL}}_\mu = (\mathcal{L}^\epsilon)^{-1}\cdot \mathrm{CURL}^\dagger \cdot \mathcal{S}^{\frac{1}{\mu}}\,, \tag{4.38} $$

where $\mathcal{S}^{\frac{1}{\mu}}$ corresponds to the modified inner product in the space $\mathcal{HS}$ and

$$ \left({}_\epsilon\overline{\mathrm{CURL}}_\mu\,\vec{B},\,\vec{E}\right)^{\epsilon}_{\mathcal{HL}} = \left(\mathrm{CURL}\,\vec{E},\,\vec{B}\right)^{\frac{1}{\mu}}_{\mathcal{HS}} \tag{4.39} $$

by definition.

In this paper we consider problems where the tangential components of $\vec{E}$ are given on the boundary. There are other types of boundary conditions, such as impedance boundary conditions, where tangential components $[\vec{H}\times\vec{n}]$ must be approximated on the boundary. For these case the boundary integral in the identity

$$ \int_V (\mathbf{curl}\,\vec{E},\,\vec{H})\,dV = \int_V (\vec{E},\,\mathbf{curl}\,\vec{H})\,dV + \oint_{\partial V} (\vec{E},\,[\vec{H}\times\vec{n}])\,dS \tag{4.40} $$

does not vanish. The operator $\mathbf{curl}\,\vec{E}$ is adjoint to the operator which is $\mathbf{curl}\,\vec{H}$ in the interior and is the tangential component of $\vec{H}$ on the boundary. For these types of boundary conditions we must also introduce an inner product in the space $\mathcal{HL}$ which includes the boundary integral.

4.2.4. Properties of Adjoint Discrete Operators. We will apply two of the discrete vector analysis theorems for adjoint operators proven in [22],

$\overline{\mathrm{DIV}}\vec{A}=0$ if and only if $\vec{A}=\overline{\mathrm{CURL}}\,\vec{B}$, where $\vec{A}\in\mathcal{HL}$ and $\vec{B}\in\mathcal{HS}$;

$\overline{\mathrm{CURL}}\,\vec{A}=0$ if and only if $\vec{A}=\overline{\mathrm{GRAD}}\,U$, where $\vec{A}\in\mathcal{HS}$ and $U\in HC$.

To verify that Gauss's law holds in the discrete case we confirm that $\overline{\mathrm{DIV}}^\epsilon \cdot_\epsilon \overline{\mathrm{CURL}}_\mu = 0$ by noting

$$ \begin{aligned} \overline{\mathrm{DIV}}^\epsilon \cdot_\epsilon \overline{\mathrm{CURL}}_\mu &= -N^{-1}\cdot \mathrm{GRAD}^\dagger\cdot\mathcal{L}^\epsilon\cdot(\mathcal{L}^\epsilon)^{-1}\cdot\mathrm{CURL}^\dagger\cdot\mathcal{S}_\mu \\ &= -N^{-1}\cdot\mathrm{GRAD}^\dagger\cdot\mathrm{CURL}^\dagger\cdot\mathcal{S}_\mu\,, \end{aligned} $$

and

$$ \mathrm{GRAD}^\dagger\cdot\mathrm{CURL}^\dagger \equiv 0\,. \tag{4.41} $$

5. Finite-Difference Scheme.

5.1. Maxwell's curl Equations. We first consider the discrete space-continuous time equations

$$ \frac{\partial\vec{B}}{\partial t} = -\mathrm{CURL}\,\vec{E}\,, \tag{5.1-a} $$

$$ \frac{\partial\vec{E}}{\partial t} = {}_\epsilon\overline{\mathrm{CURL}}_\mu\,\vec{B}\,, \tag{5.1-b} $$

The electric and magnetic part of the energy can be expressed in terms of our primary variables $\vec{E}$ and $\vec{B}$ as

$$ \int_V (\vec{D},\,\vec{E})\,dV = \int_V \epsilon\,(\vec{E},\,\vec{E})\,dV\,, \tag{5.2-a} $$

$$ \int_V (\vec{B},\,\vec{H})\,dV = \int_V \frac{1}{\mu}\,(\vec{B},\,\vec{B})\,dV\,. \tag{5.2-b} $$

The integrals in right sides of these equations are approximated by the weighted inner products $(\vec{E},\, \vec{E})^{\epsilon}_{\mathcal{HL}}$ and $(\vec{B},\, \vec{B})^{\frac{1}{\mu}}_{\mathcal{HL}}$.

The discrete analog of the electromagentic energy is

$$\mathcal{E}^h_{EH} = (\vec{E},\, \vec{E})^{\epsilon}_{\mathcal{HL}} + (\vec{B},\, \vec{B})^{\frac{1}{\mu}}_{\mathcal{HL}}\,. \tag{5.3}$$

Taking the inner product $(\cdot,\, \cdot)^{\frac{1}{\mu}}_{\mathcal{HS}}$ of $\vec{B}$ with both sides of 5.1-a and similarly for 5.1-b we obtain

$$(\frac{\partial \vec{B}}{\partial t},\, \vec{B})^{\frac{1}{\mu}}_{\mathcal{HS}} = -(\mathrm{CURL}\, \vec{E},\, \vec{B})^{\frac{1}{\mu}}_{\mathcal{HS}}\,, \tag{5.4-a}$$

$$(\frac{\partial \vec{E}}{\partial t},\, \vec{E})^{\epsilon}_{\mathcal{HL}} = ({}_{\epsilon}\overline{\mathrm{CURL}}_{\mu}\, \vec{B},\, \vec{E})^{\epsilon}_{\mathcal{HL}}\,. \tag{5.4-b}$$

By adding these two equations,

$$\frac{\partial \mathcal{E}^h_{EH}}{\partial t} = -(\mathrm{CURL}\, \vec{E},\, \vec{B})^{\frac{1}{\mu}}_{\mathcal{HS}} + ({}_{\epsilon}\overline{\mathrm{CURL}}_{\mu}\, \vec{B},\, \vec{E})^{\epsilon}_{\mathcal{HL}}\,, \tag{5.5}$$

and using 4.39 we note that the right side of this equation is zero. This corresponds to the preservation of energy when tangential component of $\vec{E}$ is zero on the boundary. For the general case, in correspondence with 1.5, the right side of the equation will be equal to a discrete approximation of the boundary integral in 2.19. This conservation of electromagnetic energy for the discrete model is the result of the consistent and compatible construction of the discrete curl operators.

Time discretization is

$$\frac{\vec{B}^{n+1} - \vec{B}^{n}}{\Delta t} = -\mathrm{CURL}\, \vec{E}^{\alpha_1}\,, \tag{5.6-a}$$

$$\frac{\vec{E}^{n+1} - \vec{E}^{n}}{\Delta t} = {}_{\epsilon}\overline{\mathrm{CURL}}_{\mu}\, \vec{B}^{\alpha_2}\,, \tag{5.6-b}$$

where $\vec{E}^{\alpha_1} = \alpha_1\, \vec{E}^{n+1} + (1-\alpha_1)\, \vec{E}^{n}$ and $\vec{B}^{\alpha_2} = \alpha_2\, \vec{B}^{n+1} + (1-\alpha_2)\, \vec{B}^{n}$, and $t_n = \Delta t\, n$, includes both explicit and implicit methods.

Traditionally, because system of curls equations is hyperbolic, either the stable explicit method ($\alpha_1 = 0$ or $\alpha_2 = 0$) or the explicit standard standard leapfrog method [34], [38] is used. The explicit schemes do not preserve energy. For some problems, especially for problems with strongly discontinuous coefficients, it is very important to preserve energy. The only scheme of form 5.6-a, 5.6-b which preserves energy is the second order implicit midpoint method ($\alpha_1 = \alpha_2 = 0.5$). Also, there are situations when the increased stability of an implicit method is necessary to avoid taking extremely small time step. This situation occurs when computing the motion of fully electromagnetic particles in the implosion of a laser fusion capsule [1].

To prove that midpoint method is conservative take the inner product of equation 5.6-a with $\vec{B}^{0.5}$ and second equation with $\vec{E}^{0.5}$ we get

$$\frac{\left(\mathcal{E}^h_{EH}\right)^{n+1} - \left(\mathcal{E}^h_{EH}\right)^{n}}{\Delta t} = \tag{5.7}$$
$$-(\mathrm{CURL}\, \vec{E}^{0.5},\, \vec{B}^{0.5})^{\frac{1}{\mu}}_{\mathcal{HS}} + ({}_{\epsilon}\overline{\mathrm{CURL}}_{\mu}\, \vec{B}^{0.5},\, \vec{E}^{0.5})^{\epsilon}_{\mathcal{HL}}\,.$$

By construction the right-hand side of this equation reduces to discrete analog of boundary integral and guarantees the method is conservative. The method will not be conservative for any other choice of α's and conservation error will be $O(\Delta t)$.

The discrete form of the "divergence-free" conditions 2.8-a, 2.8-b is

$$\overline{\mathrm{DIV}}^{\epsilon}\, \vec{E}^{n} = 0\,, \tag{5.8-a}$$

$$\mathrm{DIV}\, \vec{B}^{n} = 0\,, \tag{5.8-b}$$

where $\overline{\mathrm{DIV}}^{\epsilon}$ and DIV are defined by equations 4.30 and 4.4 respectively.

To prove that if 5.8-a, 5.8-b are satisfied initially, then they will be satisfied at later times we first apply DIV to both sides of equation 5.6-a,

$$\frac{\mathrm{DIV}\, \vec{B}^{n+1} - \mathrm{DIV}\, \vec{B}^{n}}{\Delta t} = -\mathrm{DIV}\,\mathrm{CURL}\, \vec{E}^{\alpha_1} = 0\,. \tag{5.9}$$

The right-hand side is zero because of the properties of DIV and CURL (described in Section 4.1.4, and [21]). Therefore

$$\mathrm{DIV}\, \vec{B}^{n+1} = \mathrm{DIV}\, \vec{B}^{0} = 0\,. \tag{5.10}$$

Similarly applying $\overline{\mathrm{DIV}}^{\epsilon}$ to 5.6-b and using the results from Section 4.2.4,

$$\overline{\mathrm{DIV}}^{\epsilon}\, \vec{E}^{n+1} = \overline{\mathrm{DIV}}^{\epsilon}\, \vec{E}^{0} = 0\,. \tag{5.11}$$

The TM-mode equations for the $BS\xi$, $BS\eta$ components of the magnetic field and the $EL\zeta$ component of electric field are

$$\begin{aligned}
&\frac{BS\xi^{n+1} - BS\xi^{n}}{\Delta t} = -\, R_{13}\, EL\zeta^{\alpha_1}\,,\\
&\frac{BS\eta^{n+1} - BS\eta^{n}}{\Delta t} = -\, R_{23}\, EL\zeta^{\alpha_1}\,,\\
&L^{\epsilon}_{33}\, \frac{EL\zeta^{n+1} - EL\zeta^{n}}{\Delta t} =\\
&\left(R\dagger_{13} \cdot S^{\frac{1}{\mu}}_{11} + R^{\dagger}_{23} \cdot S^{\frac{1}{\mu}}_{21}\right) BS\xi^{\alpha_2} + \left(R\dagger_{13} \cdot S^{\frac{1}{\mu}}_{12} + R^{\dagger}_{23} \cdot S^{\frac{1}{\mu}}_{22}\right) BS\eta^{\alpha_2}\,.
\end{aligned}$$

The TE-mode equations for the $BS\zeta$ component of the magnetic field and the $EL\xi$, $EL\eta$ components of the electric field are

$$\begin{aligned}
&\frac{BS\zeta^{n+1} - BS\zeta^{n}}{\Delta t} = -\left(R_{31}\, EL\xi^{\alpha_1} + R_{32}\, EL\eta^{\alpha_1}\right)\,,\\
&L^{\epsilon}_{11}\, \frac{EL\xi^{n+1} - EL\xi^{n}}{\Delta t} + L^{\epsilon}_{12}\, \frac{EL\eta^{n+1} - EL\eta^{n}}{\Delta t} = R^{\dagger}_{31}\, S^{\frac{1}{\mu}}_{33}\, BS\zeta^{\alpha_2}\,,\\
&L^{\epsilon}_{21}\, \frac{EL\xi^{n+1} - EL\xi^{n}}{\Delta t} + L^{\epsilon}_{22}\, \frac{EL\eta^{n+1} - EL\eta^{n}}{\Delta t} = R^{\dagger}_{32}\, S^{\frac{1}{\mu}}_{33}\, BS\zeta^{\alpha_2}\,.
\end{aligned}$$

5.2. Magnetic Diffusion Equations. The finite-difference equations for equations of magnetic field diffusion are

$$\frac{\vec{B}^{n+1} - \vec{B}^{n}}{\Delta t} = -\mathrm{CURL}\, \vec{E}^{\alpha_1}\,, \tag{5.12-a}$$

$$\vec{E}^{n+1} = {}_{\sigma}\overline{\mathrm{CURL}}_{\mu}\, \vec{B}^{n+1}\,. \tag{5.12-b}$$

The TM-mode equations are

$$\frac{BS\xi^{n+1} - BS\xi^{n}}{\Delta t} = -\,R_{13}\,EL\zeta^{\alpha_1}\,,$$
$$\frac{BS\eta^{n+1} - BS\eta^{n}}{\Delta t} = -\,R_{23}\,EL\zeta^{\alpha_1}\,,$$
$$L_{33}^{\sigma}\,EL\zeta^{n+1} =$$
$$\left(R\,\dagger_{13}\cdot S_{11}^{\frac{1}{\mu}} + R_{23}^{\dagger}\cdot S_{21}^{\frac{1}{\mu}}\right)\,BS\xi^{\alpha_2} + \left(R\,\dagger_{13}\cdot S_{12}^{\frac{1}{\mu}} + R_{23}^{\dagger}\cdot S_{22}^{\frac{1}{\mu}}\right)\,BS\eta^{\alpha_2}\,.$$

The TE-mode equations are

$$\frac{BS\zeta^{n+1} - BS\zeta^{n}}{\Delta t} = -\,(\,R_{31}\,EL\xi^{\alpha_1} + R_{32}\,EL\eta^{\alpha_1})\,,$$
$$L_{11}^{\sigma}\,EL\xi^{n+1} + L_{12}^{\sigma}\,EL\eta^{n+1} = R_{31}^{\dagger}\,S_{33}^{\frac{1}{\mu}}\,BS\zeta^{\alpha_2}\,,$$
$$L_{21}^{\sigma}\,EL\xi^{n+1} + L_{22}^{\sigma}\,EL\eta^{n+1} = R_{32}^{\dagger}\,S_{33}^{\frac{1}{\mu}}\,BS\zeta^{\alpha_2}\,. \tag{5.13}$$

5.3. Orthogonal Grids. To demonstrate how discrete equations looks like on rectangular grid we will write down explicit form of discrete magnetic diffusion equations. On rectangular grid with constant spacing h_x and h_y, both operators $\mathcal{L}^{\epsilon}$ and $\mathcal{S}^{\frac{1}{\mu}}$ are diagonal.

The TM-mode equations are

$$\frac{BS\xi^{n+1}_{i,j+1/2} - BS\xi^{n}_{i,j+1/2}}{\Delta t} = -\frac{EL\zeta^{\alpha_1}_{i,j+1} - EL\zeta^{\alpha_1}_{i,j}}{h_y}\,,$$
$$\frac{BS\eta^{n+1}_{i+1/2,j} - BS\xi^{n}_{i+1/2,j}}{\Delta t} = +\frac{EL\zeta^{\alpha_1}_{i+1,j} - EL\zeta^{\alpha_1}_{i,j}}{h_x}\,,$$
$$\tilde{\sigma}_{i,j}EL\zeta^{n+1}_{i,j} = \frac{\frac{BS\eta^{n+1}_{i+1/2,j}}{\tilde{\mu}_{i+1/2,j}} - \frac{BS\eta^{n+1}_{i-1/2,j}}{\tilde{\mu}_{i-1/2,j}}}{h_x} - \frac{\frac{BS\xi^{n+1}_{i,j+1/2}}{\tilde{\mu}_{i,j+1/2}} - \frac{BS\xi^{n+1}_{i,j-1/2}}{\tilde{\mu}_{i,j-1/2}}}{h_y}$$

where

$$\tilde{\sigma}_{i,j} = \frac{1}{4}\sum_{k=\pm\frac{1}{2},l=\pm\frac{1}{2}} \sigma_{i+k,j+l}\,,$$
$$\tilde{\mu}_{i,j+1/2} = \frac{1}{2}\left(\frac{1}{\mu_{i+1/2,j+1/2}} + \frac{1}{\mu_{i-1/2,j+1/2}}\right)^{-1}\,,$$
$$\tilde{\mu}_{i+1/2,j} = \frac{1}{2}\left(\frac{1}{\mu_{i+1/2,j+1/2}} + \frac{1}{\mu_{i+1/2,j-1/2}}\right)^{-1}\,.$$

We see that our approach gives the well-known harmonic means for μ. This is appropriate average to ensure the continuity of normal component of $\vec{B}$. For σ we have the arithmetic mean, which guarantees continuity of tangential component of $\vec{E}$.

The TE-mode equations are

$$\frac{BS\zeta^{n+1}_{i,j} - BS\zeta^{n}_{i,j}}{\Delta t} =$$

$$\frac{EL\xi^{\alpha_1}_{i+1/2,j+1} - EL\xi^{\alpha_1}_{i+1/2,j}}{h_y} - \frac{EL\eta^{\alpha_1}_{i+1,j+1/2} - EL\xi^{\alpha_1}_{i,j+1/2}}{h_x},$$

$$\tilde{\sigma}_{i+1/2,j}\, EL\xi^{n+1}_{i+1/2,j} = \frac{\frac{BS\zeta^{n+1}_{i+1/2,j+1/2}}{\mu_{i+1/2,j+1/2}} - \frac{BS\zeta^{n+1}_{i+1/2,j-1/2}}{\mu_{i+1/2,j-1/2}},}{h_y},$$

$$\tilde{\sigma}_{i,j+1/2}\, EL\eta^{n+1}_{i,j+1/2} = -\frac{\frac{BS\zeta^{n+1}_{i+1/2,j+1/2}}{\mu_{i+1/2,j+1/2}} - \frac{BS\zeta^{n+1}_{i-1/2,j+1/2}}{\mu_{i-1/2,j+1/2}},}{h_x},$$

where

$$\tilde{\sigma}_{i,j+1/2} = \frac{1}{2}\left(\sigma_{i+1/2,j+1/2} + \sigma_{i-1/2,j+1/2}\right),$$
$$\tilde{\sigma}_{i+1/2,j} = \frac{1}{2}\left(\sigma_{i+1/2,j+1/2} + \sigma_{i+1/2,j-1/2}\right), .$$

Therefore, on orthogonal grids our method reduces to the standard appropriate method.

Therefore, we can conclude that for orthogonal grids our method gives well-known treatment of discontinuous coefficients.

6. Solution Procedure. When $\alpha_1,\, \alpha_2 \neq 0$ then our method is implicit and on every time step we must solve system of linear equations 5.6-a, 5.6-b. This system can be written as

$$\vec{B}^{n+1} = -\Delta t\, \alpha_1\, \mathrm{CURL}\, \vec{E}^{n+1} + \vec{F}_B(\vec{B}^n,\, \vec{E}^n)\,, \tag{6.1}$$
$$\mathcal{L}^\epsilon\, \vec{E}^{n+1} = \Delta t\, \alpha_2\, \mathrm{CURL}^\dagger \cdot \mathcal{S}^{\frac{1}{\mu}}\, \vec{B}^{n+1} + \vec{F}_E(\vec{B}^n,\, \vec{E}^n)\,, \tag{6.2}$$

where

$$\vec{F}_B(\vec{B}^n,\, \vec{E}^n) = \vec{B}^n - \Delta t\, (1-\alpha_1)\, \mathrm{CURL}\, \vec{E}^n\,, \tag{6.3}$$
$$\vec{F}_E(\vec{B}^n,\, \vec{E}^n) = \mathcal{L}^\epsilon \vec{E}^n + \Delta t\, (1-\alpha_2)\, \mathrm{CURL}^\dagger \cdot \mathcal{S}^{\frac{1}{\mu}}\, \vec{B}^n\,, \tag{6.4}$$

are known. Even for nonuniform grids, we can easily eliminate $\vec{B}^{n+1}$ and obtain single second-order equation for $\vec{E}$;

$$\mathcal{A}\, \vec{E}^{n+1} \stackrel{def}{=} \left(\mathcal{L}^\epsilon + (\Delta t)^2\, \alpha_1\, \alpha_2\, \mathrm{CURL}^\dagger \cdot \mathcal{S}^{\frac{1}{\mu}} \cdot \mathrm{CURL}\right)\, \vec{E}^{n+1} = \vec{F}(\vec{B}^n, \vec{E}^n)\,, \tag{6.5}$$

where

$$\vec{F}(\vec{B}^n,\, \vec{E}^n) = \vec{F}_E(\vec{B}^n,\, \vec{E}^n)\,, + \Delta t\, \alpha_2 \mathrm{CURL}^\dagger \cdot \mathcal{S}^{\frac{1}{\mu}}\, \vec{F}_B(\vec{B}^n, \vec{E}^n) \tag{6.6}$$

is known. The operator $\mathcal{A}$ defined by 6.5 is SPD, which follows from its structure and properties of operators $\mathcal{L}^\epsilon$ and $\mathcal{S}^{\frac{1}{\mu}}$.

Equation 6.5 contains both the TM and TE modes. The TM equation is a “scalar” equation for $EL\zeta$ and can be solved effectively by any preconditioned iterative method which takes advantage of SPD property. The TE equation is a block, (2×2) SPD system for $EL\xi$ and $EL\eta$ with a structure of this system is very close to system arising for the heat flux in the heat conduction equation solved in [49], [25], and [41], and one can use the iterative methods described in these papers to solve this system.

Once 6.5 has been solved, $\vec{B}^{n+1}$ is explicitly defined by 6.1. This solution procedure guarantees that the discrete analog of Faraday's law is satisfied exactly, independent of how accurate 6.5 is solved (see, [47] for a general discussion on violation of conservation properties when solving difference equations by iterative methods).

7. Numerical Examples. In this section, we demonstrate the effectiveness of our approach for solving Maxwell's curl equations for the TE mode and the equations of magnetic diffusion for the TM mode.

7.1. Maxwell's curl Equations. We integrate Maxwell's curl equations with conservative mid-point method ($\alpha_1 = \alpha_2 = 0.5$) and a time step sufficiently small so the time errors are much smaller than the spatial discretization errors. All the parameters in this subsection are given in MKS units and the free space constants are $\epsilon_0 = 8.85 \times 10^{-12}$, and $\mu_0 = 1.2566 \times 10^{-6}$.

7.1.1. Reflection and Refraction at the Boundary of Two Nonconducting Media: Normal Incidence. The reflection and refraction of the pulse at the boundary of two nonconducting media ([44], pp. 382–385) is one dimensional problem when the incident pulse is normal to the interface. We solve this problem in a 2D rectangular domain $[-1, 1] \times [0, 1]$, where interface between two media coincides with the y axis.

The permitivities in the "left" and "right" media are $\epsilon_1 = k_1\,\epsilon_0$, $\epsilon_2 = k_2\,\epsilon_0$, and $\mu = \mu_0$ for both media. The indices of refraction are $n_1 = \sqrt{k_1}$, $n_2 = \sqrt{k_2}$. In our calculations we took $k_1 = 1$ and $k_2 = 2$.

The incident wave is

$$E_y^{inc}(x,t) = A_E^{inc}\, g((t - \sqrt{\mu_0\,\epsilon_1}\,(x+1)) * 10^9)\,, \tag{7.1-a}$$

$$H_z^{inc}(x,t) = A_H^{inc}\, g((t - \sqrt{\mu_0\,\epsilon_1}\,(x+1)) * 10^9)\,, \tag{7.1-b}$$

where g is the pulse function

$$g(s) = \left\{ \begin{array}{ll} 1 - \cos(2\,\pi\,s)\,, & 0 \le s \le 1 \\ 0 \quad \text{elsewhere} & \end{array} \right. , \tag{7.2}$$

and the amplitudes are

$$A_E^{inc} = 0.5\,\sqrt{\frac{\mu_0}{\epsilon_1}}\,, \quad A_H^{inc} = A_E^{inc}\,n_1\,\sqrt{\frac{\epsilon_0}{\mu_0}}\,. \tag{7.3}$$

This wave is generated by imposing boundary conditions for E_y at $x = -1$

$$E_y|_{x=-1} = A_E^{inc}\, g(t * 10^9)\,. \tag{7.4}$$

The incident wave reaches the boundary between the two materials at time $t^* = \sqrt{\mu_0\,\epsilon_1} = 3.3348 * 10^{-9}$.

The reflected wave

$$E_y^{ref}(x,t) = A_E^{ref}\, g((t + \sqrt{\mu_0\,\epsilon_1}\,(x-1)) * 10^9)\,, \tag{7.5-a}$$

$$H_z^{ref}(x,t) = A_H^{ref}\, g((t + \sqrt{\mu_0\,\epsilon_1}\,(x-1)) * 10^9)\,, \tag{7.5-b}$$

has the amplitudes

$$A_E^{ref} = -A_E^{inc}\,\frac{n_2 - n_1}{n_1 + n_2}\,, \quad A_H^{ref} = A_E^{ref}\,n_1\,\sqrt{\frac{\epsilon_0}{\mu_0}}\,. \tag{7.6}$$

The transmitted wave

$$E_y^{tran}(x,t) = A_E^{tran}\, g((t - \sqrt{\mu_0\,\epsilon_2}\,(x + \frac{k_1}{k_2})) * 10^9)\,, \tag{7.7-a}$$

$$H_z^{tran}(x,t) = A_H^{tran}\, g((t - \sqrt{\mu_0\,\epsilon_2}\,(x + \frac{k_1}{k_2})) * 10^9)\,, \tag{7.7-b}$$

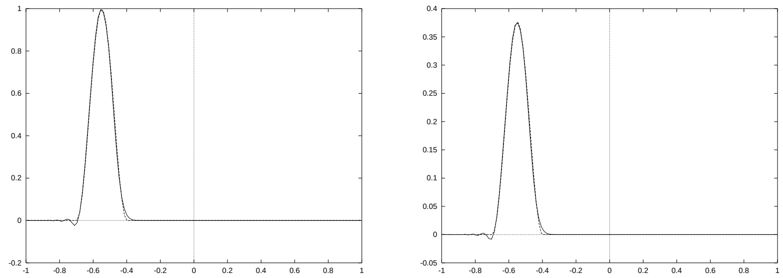

FIG. 9. *Exact and 1-D approximate solution ($M = 129$) for $t = 2 \times 10^{-9}$. Left – H_z component of magnetic field, right – E_y component of electric field.*

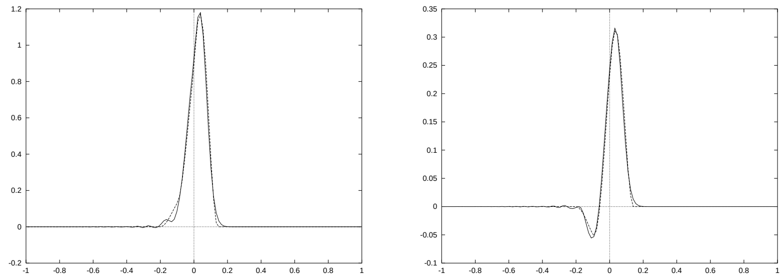

FIG. 10. *Exact and 1-D approximate solution ($M = 129$ for $t = 4 \times 10^{-9}$. Left – H_z component of magnetic field, right – E_y component of electric field.*

has the amplitudes

$$A_E^{tran} = A_E^{inc} \frac{2\, n_1}{n_1 + n_2}\,, \quad A_H^{tran} = A_E^{tran}\, n_2 \sqrt{\frac{\epsilon_0}{\mu_0}} \tag{7.8}$$

Until the transmitted or reflected waves reach the computational boundaries the exact solution for the "left" media, $-1 \le x \le 0$, is the sum of incident wave and reflected wave and for "right" media, $0 \le x \le 1$, is the transmitted wave.

The exact and 1-D approximate solution ($M = 129$), which plays the reference role for 2-D computations, for the characteristic time moments are presented in Figs. 9-11 The numerical method accurately approximates the pulse traveling in a homogeneous media ($t = 2 \times 10^{-9}$, Fig. 9), during the interaction with the discontinuity ($t = 4 \times 10^{-9}$, Fig. 10) and the shape and velocity of the transmitted and reflected waves (time, $t = 6 \times 10^{-9}$, Fig. 11).

In two dimensions, because this example is posed for the TE mode, the magnetic field has just one component H_z which is measured in the center of the 2-D cell. Because μ is also given in center of the cell, we can easily extract H_z from $B_z = \mu\, H_z$, which is our primary variable in numerical method.

We solved this problem on both smooth and random grids, Fig. 12. The smooth grid is obtained by mapping a of uniform grid in rectangular $[-1\,,1] \times [0\,,1]$ in $(\xi,\, \eta)$ domain into the same computational space $x(\xi\,,\eta)\,, y(\xi\,,\eta)$ by

$$x(\xi,\, \eta) = \xi + 0.1\, \sin(2\,\pi\,\xi)\, \sin(2\,\pi\,\eta)\,, \quad y(\xi,\, \eta) = \eta + 0.1\, \sin(2\,\pi\,\xi)\, \sin(2\,\pi\,\eta)\,.$$

The nonsmooth grid (random grid), is obtained by moving nodes in a uniform square

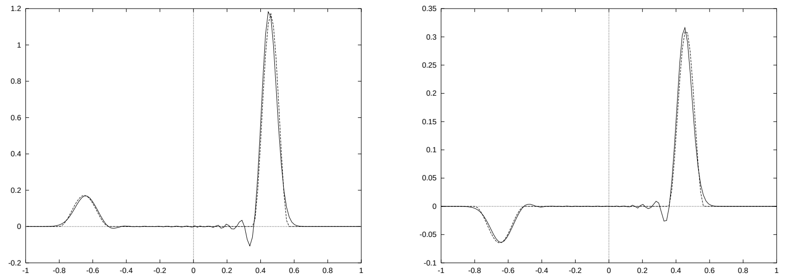

FIG. 11. *Exact and 1-D approximate solution ($M = 129$) for $t = 6\times10^{-9}$. Left – H_z component of magnetic field, right – E_y component of electric field.*

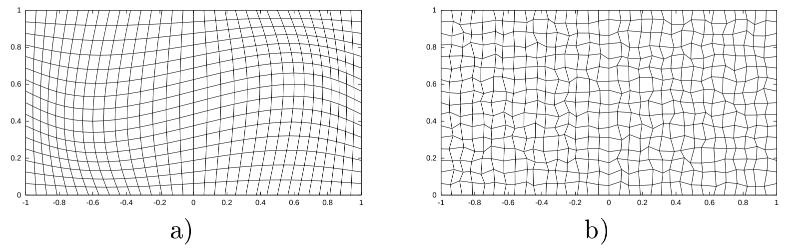

FIG. 12. *Computational grids (33×17); a) Smooth grid, b) Random grid.*

grid in random directions and with a random amplitude equal to 20% of initial grid size.

To measure the accuracy of the 2-D calculations, we compare the values of H_z as a function of time for the 1-D and 2-D calculations at a fixed position. In 1-D we plot the solution at the cell center closest to $x = 0.1$. In 2-D we plot the solution at the cell center closest to $(0.1, 0)$. These values plotted in Fig. 13 and Fig. 14 demonstrate that behavior of 1-D and 2-D solutions are close.

In Fig. 15 the straight contour lines illustrate how well the 2-D approximate solution for H_z preserves the one dimensional shape on the nonuniform smooth grid.

We also calculated the convergence rate in the discrete max and L_2 norms on a sequence of refined grids. The error for $H_z = H\zeta$ is defined as

$$\Psi^H_{i+1/2,j+1/2} = H\zeta_{i+1/2,j+1/2} - H\zeta^{exact}(x^c_{i+1/2,j+1/2}, y^c_{i+1/2,j+1/2})\,, \tag{7.9}$$

where $(x^c_{i,j},\, y^c_{i,j})$ is the geometrical center of $(i + 1/2, j + 1/2)$ cell. The norms of Ψ_H are defined as

$$||\Psi^H||_{\max} = \max_{i,j} \Psi^H_{i,j}\,, \tag{7.10-a}$$

$$||\Psi^H||_{L_2} = \sqrt{\sum_{i,j} \left(\Psi^H_{i+1/2,j+1/2}\right)^2 VC_{i+1/2,j+1/2}}\,. \tag{7.10-b}$$

For $\vec{E} = (EL\xi, EL\eta)$ the errors are defined as

$$\Psi^{EL\xi}_{i+1/2,j} = EL\xi_{i+1/2,j} - EL\xi^{exact}(x^\xi_{i+1/2,j}, y^\xi_{i+1/2,j})\,, \tag{7.11-a}$$

$$\Psi^{EL\eta}_{i,j+1/2} = EL\xi_{i,j+1/2} - EL\eta^{exact}(x^\eta_{i,j+1/2}, y^\eta_{i,j+1/2})\,, \tag{7.11-b}$$

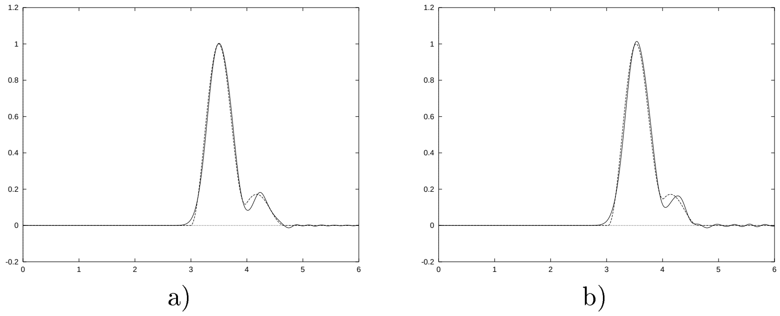

FIG. 13. *Component H_z as function of time; a) 1-D case, $M = 129$, b) 2-D case, smooth grid, $M = 129$, $N = 65$*

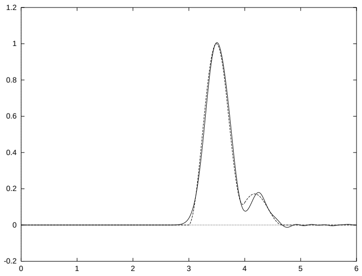

FIG. 14. *Component H_z as function of time for 2-D case, random grid, $M = 129$, $N = 65$*

where $EL\xi^{exact}$ and $EL\eta^{exact}$ are projections of the exact solution to the edges, $(x^{\xi}_{i+1/2,j}, y^{\xi}_{i+1/2,j})$ and $(x^{\eta}_{i,j+1/2}, y^{\eta}_{i,j+1/2})$ are the coordinates of the mid-points of the edges. The norms for $\vec{\Psi}^E = (\Psi^{EL\xi}, \Psi^{EL\eta})$ are defined as follows

$$||\vec{\Psi}^E||_{\max} = \max_{i,j} \left[\max \left(\Psi^{EL\xi}_{i+1/2,j}, \Psi^{EL\eta}_{i,j+1/2} \right) \right] , \tag{7.12-a}$$

$$||\vec{\Psi}^E||_{L_2} = \sqrt{(\vec{\Psi}^E, \vec{\Psi}^E)_{\mathcal{HL}}} \, . \tag{7.12-b}$$

In Table i, we see that at $t = 2 \times 10^{-9}$, the L_2 and max norm convergence rates for both smooth and random grids are between first- and second-order. At $t = 4 \times 10^{-9}$ (Table ii) the convergence rates are similar, but the solution is less accurate because of a errors introduced when the wave interacted with the discontinuity. At $t = 6 \times 10^{-9}$ (Table iii) the errors are much larger on the coarse grid because there are insufficient mesh points to resolve the transmitted wave. Our convergence analysis for the 1-D case (not presented here) is in close agreement with these 2-D results.

These results verify the effectiveness of the method for problems with discontinuous coefficients on nonsmooth, nonorthogonal grids.

7.2. Scattering of a Plane Wave on Perfect Conductor. Our next example is an infinite domain problem modeling the scattering of a plane wave on a perfect conductor [34], [38]. We consider a plane wave

$$\vec{E}(x,t) = \begin{pmatrix} 0 \\ \sqrt{\mu_0/\epsilon_0}\, g((t - (x+0.1)\sqrt{\epsilon_0\,\mu_0})\, 10^9) \end{pmatrix} \tag{7.13-a}$$

$$H_z(x,t) = g((t - (x+0.1)\sqrt{\epsilon_0\,\mu_0})\, 10^9) \tag{7.13-b}$$

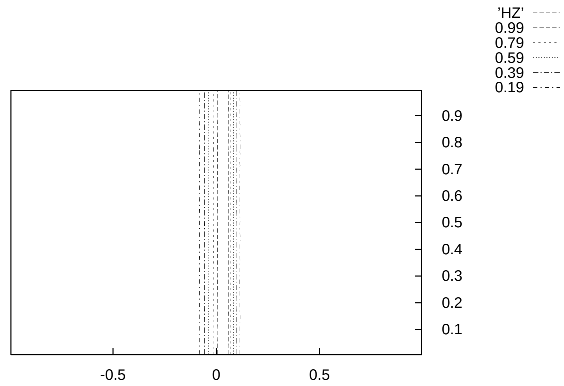

FIG. 15. *Isolines of H_z at $t = 4$, for smooth grid, $M = 129$, $N = 65$.*

Grid	Smooth		Non-smooth	
M/N	$\vec{H}$	$\vec{E}$	$\vec{H}$	$\vec{E}$
33/17	0.108	4.08E-2	0.142	5.11E-2
	0.322	0.115	0.421	0.124
65/33	3.34E-2	1.27E-2	4.42E-2	1.71E-2
	0.117	4.26E-2	0.13	5.68E-2
129/65	9.80E-3	3.72E-3	1.25E-2	4.93E-3
	3.79E-2	1.34E-2	4.42E-2	2.08E-2
L_2	1.76	1.77	1.82	1.74
Max	1.62	1.66	1.55	1.44

TABLE I

The errors for wave reflection and refraction at the boundary of two nonconducting media at $t = 2 \times 10^{-9}$. For each grid size in top sub-row we present L_2 error, and in bottom sub-row we present max error. In the very bottom we present estimation for convergence rate for both norms.

Grid	Smooth		Non-smooth	
M/N	$\vec{H}$	$\vec{E}$	$\vec{H}$	$\vec{E}$
33/17	0.209	8.09E-2	0.199	8.26E-2
	0.532	0.230	0.484	0.219
65/33	9.13E-2	3.23E-2	9.19E-2	3.21E-2
	0.307	0.110	0.250	0.105
129/65	3.01E-2	8.57E-3	2.91E-2	8.42E-3
	0.120	3.30E-2	0.106	3.38E-2
L_2	1.60	1.91	1.65	1.93
Max	1.35	1.73	1.23	1.63

TABLE II

The errors for wave reflection and refraction at the boundary of two nonconducting media at $t = 4 \times 10^{-9}$. For each grid size in top sub-row we present L_2 error, and in bottom sub-row we present max error. In the very bottom we present estimation for convergence rate for both norms.

Grid	Smooth		Non-smooth	
M/N	$\vec{H}$	$\vec{E}$	$\vec{H}$	$\vec{E}$
33/17	0.283	8.12E-2	0.269	7.87E-2
	0.683	0.178	0.647	0.186
65/33	0.176	4.73E-2	0.164	4.40E-2
	0.603	0.156	0.526	0.135
129/65	6.04E-2	1.62E-2	5.35E-2	1.44E-2
	0.216	5.74E-2	0.178	4.95E-2
L_2	1.54	1.54	1.61	1.61
Max	1.48	1.44	1.56	1.44

TABLE III

The errors for wave reflection and refraction at the boundary of two nonconducting media at $t = 6 \times 10^{-9}$. For each grid size in top sub-row we present L_2 error, and in bottom sub-row we present max error. In the very bottom we present estimation for convergence rate for both norms.

incident to a perfectly conducting circular cylinder of radius 0.1m centered at the origin. Our media is "free space" with $\epsilon = \epsilon_0$ and $\mu = \mu_0$.

The numerical domain is an annulus with inner radius 0.1 m and outer radios 1.1 m. Because the problem is symmetric about the x-axis we solve the problem in the half domain

$$\Omega = \left\{ (x,y) \in (0.1 < \sqrt{x^2+y^2} < 1.1) \times (y > 0) \right\} .$$

We define the tangential component of $\vec{E}$ to be zero on all boundaries except the surface of the inner cylinder, where we define the tangential component of $\vec{E}$ equals to tangential component of the incident wave (see [34] for details). That is, we solve for the scattered (i.e., total minus incident) field. These boundary conditions are valid until $t = 4$ ns, when the boundary condition on the outer cylinder starts to generate spurious reflections. The initial conditions correspond to time when the incident wave (traveling from left to right) just arrives at the inner cylinder. Therefore, initially there are no scattered waves and the electric and magnetic fields are zero.

The problem is solved on the uniform polar grid (see, Fig. 16) with 31 nodes in r and 16 nodes in θ. In Fig. 17 the magnetic field is plotted as function of time at the two observation points indicated by box in Fig. 16. The results are almost identical with results in [38], Fig. 7. Similar to [38] we observe second order convergence in the spatial error.

7.3. Equations of Magnetic Diffusion. The equation of magnetic diffusion for TE mode is the same as 2-D heat conduction equation, where H_z plays role of temperature. Therefore the numerical examples in [48], [49] and [25] for the heat equation are also valid for the TE mode of magnetic diffusion equations. Therefore in this paper we consider only TM mode for these equation.

For simplicity, we consider $\mu = 1$ (and therefore $\vec{B} = \vec{H}$). The computational domain is square $[-0.5, 0.5] \times [-0.5, 0.5]$. The conductivity $\sigma_1 = 1$ for $x < 0$ and $\sigma_2 = 10$ for $x > 0$. The 1-D analytical solution is

$$H_x(x,y,t) = 0\,, \tag{7.14-a}$$

$$H_y(x,y,t) = e^{-4\,\pi^2\,t}\,\sqrt{\sigma}\,\sin(2\,\pi\,\sqrt{\sigma}\,x)\,, \tag{7.14-b}$$

$$E_z(x,y,t) = e^{-4\,\pi^2\,t}\,2\pi\,\cos(2\,\pi\,\sqrt{\sigma}\,x)\,. \tag{7.14-c}$$

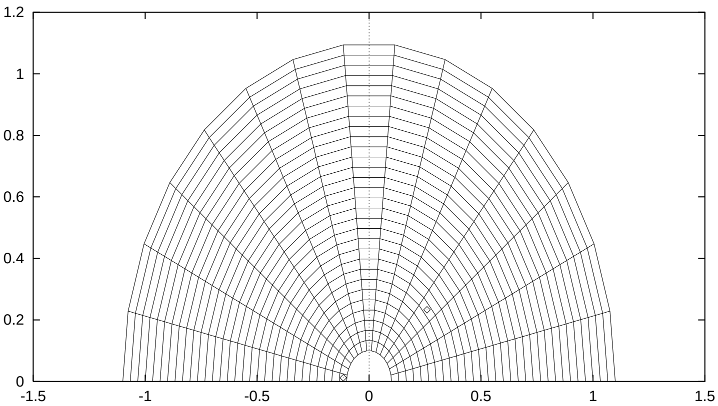

FIG. 16. *Grid and observation points* $A = (-0.115,\, 0.0121)$ *and* $B = (0.259,\, 0233)$.

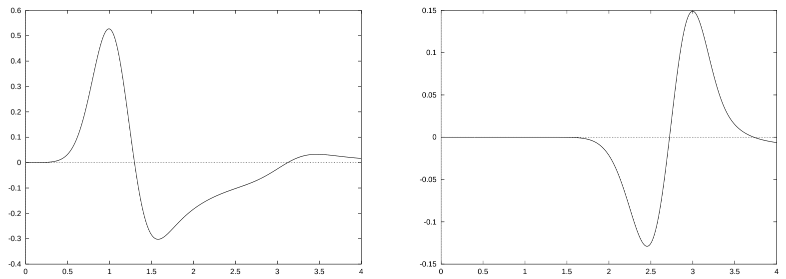

FIG. 17. H_z *as function of time in nanoseconds at points* $A = (-0.115,\, 0.0121)$ *and* $B = (0.259,\, 0233)$. *Time is scaled to ns.*

The normal component H_y of $\vec{H} = \vec{B}$ on the discontinuity line $x = 0$ is zero and therefore, is continuous. The tangential component E_z of $\vec{E}$ is also continuous on $x = 0$. The of the profiles of H_y and E_z at time $t = 0.02$ are shown in Fig.18.

The initial and boundary conditions for 2-D problem are taken from the exact solution. An example of the smooth grid is shown in Fig. 19. The nonsmooth, random grid is similar to one shown in Fig. 12 b).

The convergence rate for smooth grids is close to second-order (iv). On nonsmooth grids, the convergence rate for $\vec{E}$ is also close to second-order and less for $\vec{H}$.

8. Discussion. We have constructed mimetic FDMs for both the TE and TM modes for 2-D Maxwell's curl equations and the equations of magnetic diffusion on nonorthogonal, nonsmooth grids. Because discrete operators were derived using the discrete vector and tensor analysis developed in [21]-[24] they satisfy discrete analogs of the main theorems of vector analysis. In particular for this reason, the method does not have spurious solutions and the "divergence-free" conditions for Maxwell's equations are automatically satisfied.

The tangential components of the electric field and the normal components of magnetic flux used in FDM are continuous even across discontinuity. This choice guarantees that problems with strongly discontinuous coefficients treated properly. Furthermore on rectangular grids our method reduces to the analytically correct averaging for discontinuous coefficients. We have proved that the implicit mid-point time integration method is conservative and leads to a SPD system of linear equa-

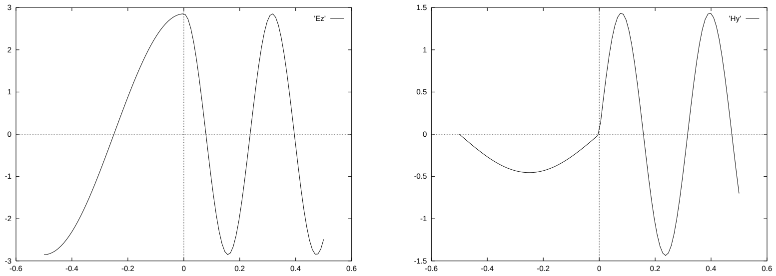

FIG. 18. *Exact solution for the diffusion problem, left – E_z, right – H_y, at $t = 0.02$.*

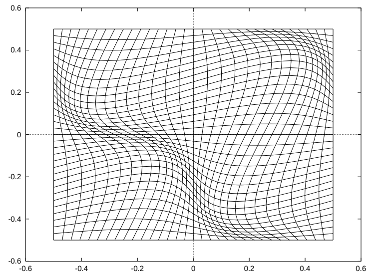

FIG. 19. *The smooth 33×33 grid used in example.*

tions. On arbitrary quadrilateral grid we have demonstrated the convergence and robustness of the method in numerical examples.

The FDM is formulated in terms of coordinate invariant quantities such as lengths, areas, volumes and angles. The method can be used in any coordinate system by expressing these quantities in terms of the particular coordinate system. Also, when ϵ, μ, and σ are tensors, the method can be used by changing the form of the $\mathcal{L}$, and $\mathcal{S}$ similar as is done for the heat equation with tensor conductivity (see, [25]).

As mentioned in Section 4.2.3, the method can be adapted for impedance boundary conditions and the resulting system of linear equations can also be proved to be SPD (prove is similar to the one given in [24]).

The extension to 3-D hexahedral grids is technically straightforward. The details are tedious and depend upon the shape chosen for faces of the 3-D grid cells. One of the standard ways of doing this is to consider tri-linear map of the reference cube to hexahedron. The extension to unstructured grids also straightforward once the cell, face and edge are well defined.

The theoretical investigation of the stability and convergence of the FDM described in this paper can be done using approach similar to the energy method used in [14], [13], [4], [19] for FDMS, or [39], [40] for finite element methods.

We are continuing to develop a discrete version of electromagnetic theory on general grids by extending the discrete theory for uniform rectangular grids [11] based on discrete vector analysis [21]-[24]. The approach will involve discrete scalar and vector potentials, which can be introduced on the base of discrete version of orthogonal decomposition theorems proved in [23]. That is, any vector $\vec{A} \in \mathcal{HS}$ can be represented uniquely as

$$\vec{A} = \overline{\mathrm{GRAD}}\,\varphi + \mathrm{CURL}\,\vec{B}\,, \tag{8.1}$$

Grid	Smooth		Non-smooth	
M=N	$\vec{H}$	$\vec{E}$	$\vec{H}$	$\vec{E}$
33	2.75E-2	2.34E-2	1.93E-2	1.60E-2
	0.107	9.46E-2	7.13E-2	4.51E-2
65	7.16E-3	6.34E-3	5.38E-3	4.21E-3
	3.57E-2	2.69E-2	1.93E-2	1.50E-2
129	1.87E-3	1.77E-3	1.79E-3	1.25E-3
	1.01E-2	6.99E-3	7.71E-3	3.74E-3
L_2	1.93	1.84	1.58	1.75
Max	1.82	1.94	1.32	2.00

TABLE IV

Errors for problem of magnetic diffusion at $t = 0.02$. For each grid size in top sub-row we present L_2 error, and in bottom sub-row we present max error. In the very bottom we present estimation for convergence rate for both norms.

where $\varphi \in HC$ and $\vec{B} \in \mathcal{HL}$, and similarly that any vector $\vec{A} \in \mathcal{HL}$ can be presented as

$$\vec{A} = \mathrm{GRAD}\,\varphi + \overline{\mathrm{CURL}}\,\vec{B}\,, \tag{8.2}$$

where $\varphi \in HN$ and $\vec{B} \in \mathcal{HS}$.

Acknowledgment. This work was performed under the auspices of the US Department of Energy (DOE) contract W-7405-ENG-36 and the DOE/BES (Bureau of Energy Sciences) Program in the Applied Mathematical Sciences contract KC-07-01-01.

The authors are thankful to D. Barnes, J. Morel, T. Oliphant Jr., S. Steinberg for many fruitful discussions.

REFERENCES

[1] A. C. Adam, A. G. Serveniere, J. C. Nedelec and P. A. Raviart, *Study of an Implicit Scheme for Integrating Maxwell's Equations*, Comput. Meth. in Appl. Mech. and Eng., 22 (1980), pp. 327–346.

[2] R. Albanese and G. Rubinacci, *Analysis of Three-Dimensional Electromagnetic Fields Using Edge Elements*, J. Comput. Phys., 108 (1993), pp. 236-245.

[3] F. Assous, P. Degond and J. Sergé, *Numerical Approximations of the Maxwell Equations in Inhomogeneous Media by P^1 Conforming Finite Element Method*, J. of Comput. Phys., 128 (1996) pp. 363-380.

[4] N. V. Ardelyan, *The Convergence of Difference Schemes for Two-Dimensional Equations of Acoustics and Maxwell's Equations*, USSR Comput. Math. and Math. Phys., 23 (1983), pp. 93–99.

[5] A. Bossavit, *A Rationale for "Edge-Elements" in 3-D Fields Computations*, IEEE Transaction of Magnetics, 24 (1988), pp. 74–79.

[6] A. Bossavit, *Computational Electromagnetism. Variational Formulations, Complementarity, Edge Elements*, Academic Press, 1998.

[7] R. C. Booton, Jr., *Computational Methods for Electromagnetics and Microwaves*, John Wiley & Sonc, Inc., New York, 1992.

[8] J. U. Brackbill and D. C. Barnes, *The Effect of Nonzero $\nabla \cdot \mathbf{B}$ on the Numerical Solution of the Magneto-hydrodynamics Equations*, J. of Comput. Phys., 35 (1980) pp. 426-430.

[9] Z. Cai, J. E. Jones, S. F. McCormick and T. F. Russell, *Control-Volume Mixed Finite Element Methods*, to appear at Computational Geosciences.

[10] Z. J. Cendes, *Vector Finite Elements for Electromagnetic Field Computation*, IEEE Transaction of Magnetics, 27 (1991), pp. 3958–3966.

[11] W. C. Chew *Electromagnetic Theory on a Lattice*, Journal of Applied Physics, 75 (1994), pp. 4843–4850.

[12] L. Demkowicz and L. Vardapetyan, *Modeling of Electromagnetic Absorption/Scattering Problems Using hp-Adaptive Finite Elements*, TICAM Report 97-02, Texas Institute for Computational and Applied Mathematics, The University of Texas at Austin, 1997.

[13] A. A. Denisov, A. V. Koldoba, Yu. A. Poveshchenko, *The Convergence to Generalized Solutions of Difference Schemes of the Reference-Operator Method for Poisson's Equation*, USSR Comput. Math. and Math. Phys., 29 (1989), pp. 32–38.

[14] M. V. Dmitrieva, A. A. Ivanov, V. F. Tishkin, and A. P. Favorskii, *Construction and Investigation of Support-Operators Finite-Difference Schemes for Maxwell Equations in Cylindrical Geometry*, Preprint Keldysh Inst. of Appl. Math. the USSR Ac. of Sc., 27 1985, (in Russian).

[15] A. A. Dezin, *Multidimensional Analysis and Discrete Models*, CRC Press, Boca Raton, Florida, 1995.

[16] A. Favorskii, V. Tishkin and M. Shashkov *Using of Topological Methods in Discrete Model Construction*, - Preprint Keldysh Inst. of Appl. Math. the USSR Ac. of Sc., 96, 1983, (In Russian).

[17] V. Girault, *Theory of a Finite Difference Methods on Irregular Networks*, SIAM J. Numer. Anal., 11 (1974), pp. 260-282.

[18] R. Gruber and J. Rappaz, *Finite Element Methods in Linear Ideal Magnetohydrodynamics*, Springer-Verlag, Berlin Heidelberg, 1985.

[19] B. Gustafsson, H.-O. Kreiss and J. Oliger, *Time Dependent Problems and Difference Methods*, A Wiley-Interscience Publication, John Wiley & Sons, Inc., 1995. Chapter 11., pp. 445–495.

[20] R. Holland, *Finite-Difference Time-Domain (FDTD) Analysis of Magnetic Diffusion*, IEEE Trans. Electromagnetic Compatibility, 36 (1994), pp. 32-39.

[21] J. M. Hyman and M. Shashkov, *Natural Discretizations for the Divergence, Gradient, and Curl on Logically Rectangular Grids*, An International Journal Computers & Mathematics with Applications, 33 (1997), pp. 81–104.

[22] J. M. Hyman and M. Shashkov, *The Adjoint Operators for the Natural Discretizations for the Divergence, Gradient, and Curl on Logically Rectangular Grids*, IMACS Journal of Applied Numerical Mathematics, 25 (1997), pp. 413–442.

[23] J. M. Hyman and M. Shashkov, *The Orthogonal Decomposition Theorems for Mimetic Finite Difference Methods*, Report LA-UR-96-4735 of Los Alamos National Laboratory, Los Alamos, New Mexico, USA, Submitted to SIAM Journal on Numerical Analysis.

[24] J. M. Hyman and M. Shashkov, *The Approximation of Boundary Conditions for Mimetic Finite Difference Methods*, Report LA-UR-97-5158 of Los Alamos National Laboratory, Los Alamos, New Mexico, USA, submitted to An International Journal Computers & Mathematics with Applications.

[25] J. M. Hyman, M. Shashkov and S. Steinberg, *The Numerical Solution of Diffusion Problems in Strongly Heterogeneous Non-Isotropic Materials*, J. of Comput. Phys., 132 (1997) pp. 130–148.

[26] J. D. Jackson, *Classical Electrodynamics*, Second ed., John Wiley & Sons, Inc., New York, 1975.

[27] B. Jiang, J. Wu and L. A. Pavinelli, *The Origin of Spurious Solutions in Computational Electromagnetics*, J. of Comput. Phys., 125, (1996), pp, 104-123.

[28] J. Jin, *The Finite Element Method in Electromagnetics*, John Wiley & Sons, Inc., New York, 1993.

[29] L. Kettunen, K. Forsman and A. Bossavit, *Formulation of the Eddy Current Problem in Multiply Connected Regions in Terms of h*, Int. J. Numer. Meth. Engng. **41** (1998), p. 935–954.

[30] T. K. Korshiya, V. F. Tishkin, A. P. Favorskii and M. J. Shashkov, *A Variational Approach to Construction of Difference Schemes for the Magnetic Diffusion Equations*, Preprint of Institute of Applied Mathematics, # 179, (1979), Moscow, Russia. (in Russian).

[31] T. K. Korshiya, V. F. Tishkin, A. P. Favorskii and M. J. Shashkov, *Flow-variational Difference Schemes for Calculating the Diffusion of a Magnetic Field*, Sov. Phys. Dokl., 25 (1980), pp. 832–834.

[32] T. K. Korshiya, V. F. Tishkin, A. P. Favorskii, and M. Yu. Shashkov, *Variational Approach to the Construction of Finite-Difference Schemes for the Diffusion Equations for Magnetic Field*, Diff. Eqns., 18 (1982), pp. 883–872.

[33] K. S. Kunz and R. J. Luebbers, *The Finite Difference Time Domain Method for Electromagnetics*, CRC Press, Boca Raton, Florida, 1993.

[34] R. L. LEE AND N. K. MADSEN, *A Mixed Finite Element Formulation for Maxwell's Equations in the Time Domain*, J. of Comput. Phys., 88, (1990), pp. 284-304.

[35] N. K. MADSEN, *Divergence Preserving Discrete Surface Integral Methods for Maxwell's Curl Equations Using Non-orthogonal Unstructured Grids*, J. of Comput. Phys., 119, (1995), pp. 34-45.

[36] A. R. MAIKOV, A. G. SVESHNIKOV AND S. A. YAKUNIN, *Mathematical Modeling of a Microwave Plasma Generator*, USSR Comput. Math. and Math. Phys., 25 (1985), pp. 149–157.

[37] C. MATTIUSSI, *An Analysis of Finite-Volume, Finite-Element, and Finite-Difference Methods Using some Concepts from Algebraic-Topology*, J. Comput. Phys., 133 (1997), pp. 289-309.

[38] P. MONK, *A Comparison of Three Mixed Methods for the Time-Dependent Maxwell's Equations*, SIAM J. Sci. Stat. Comput., 13 (1992), pp. 1097-1122.

[39] P. MONK, *Analysis of Finite Element Method for Maxwell's Equations*, SIAM Journal on Numerical Analysis, 29, (1992), pp. 714-729.

[40] P. MONK, *An Analysis of Nedelec's Method for the Spatial Discretization of Maxwell's Equations*, J. of Comp. and Appl. Math., 47 (1993), pp. 101–121.

[41] J. E. MOREL, R. M. ROBERTS AND M. SHASHKOV, *A Local Support-Operator Diffusion Discretization Scheme for Quadrilateral r-z Meshes*, Report LA-UR-97-577 of Los Alamos National Laboratory, Los Alamos, New Mexico, USA, to appear at Journal of Computational Physics.

[42] J. C. NEDELEC, *Mixed Finite Elements in R^3*, Numerische Mathematik, 35 (1980), pp. 315–341.

[43] P. A. RAVIART AND J. M. THOMAS, *A Mixed Finite Element Method for 2-nd Order Elliptic Problems*, In I. Galligani and E. Magenes, Eds., Mathematical Aspects of Finite Element Methods, pp. 292–315, Springer-Verlag, 1977.

[44] J. R. REITZ, F. J. MILFORD, AND R. W. CHRISTY, *Foundations of Electromagnetic Theory*, Third Edition, 1980. Chapters 16-18., Pages 383.

[45] A. A. SAMARSKII, V. F. TISHKIN, A. P. FAVORSKII, AND M. YU. SHASHKOV, *Operational Finite-Difference Schemes*, Diff. Eqns., 17 (1981), pp. 854–862.

[46] M. SHASHKOV, *Conservative Finite-Difference Schemes on General Grids*, CRC Press, Boca Raton, Florida, 1995.

[47] M. SHASHKOV, *Violation of Conservation Laws when Solving Difference Equations by the Iteration Methods*, U.S.S.R. Comput. Maths. Math. Phys, 22 (1982), pp. 131–139.

[48] M. SHASHKOV AND S. STEINBERG, *Support-Operator Finite-Difference Algorithms for General Elliptic Problems*, J. of Comput. Phys., 118 (1995) pp. 131–151.

[49] M. SHASHKOV AND S. STEINBERG, *Solving Diffusion Equations with Rough Coefficients in Rough Grids*, J. of Comput. Phys., 129 (1996) pp. 383–405.

[50] *Finite Elements for Wave Electromagnetics. Methods and Techniques*, Edited by P. P. Silvester and G. Pelosi, IEEE Press, New York, 1994.

[51] J. A. SHERCLIFF, *A Textbook of Magnetohydrodynamics*, Pergamon Press, Oxford, 1965, page 24.

[52] A. TAFLOVE, *Computational Electrodynamics. The Finite-Difference Time-Domain Method*, Artech House, Inc., Boston , 1995.

[53] J. P. WEBB, *Edge Elements and What They Can do for You*, IEEE Transaction of Magnetics, 29 (1993), pp. 1460–1465.

[54] K. S. YEE, *Numerical Solution of Initial Boundary Value Problems Involving Maxwell's Equations in Isotropic Media*, IEEE Trans. Antennas and Propagation, 14 (1966), pp. 302-307.